Reactions Catalyzed by the Heme Domain of Inducible Nitric Oxide Synthase: Evidence for the Involvement of Tetrahydrobiopterin in Electron Transfer†

Amy R. Hurshman‡ and Michael A. Marletta*,‡,§,||

Howard Hughes Medical Institute, Department of Medicinal Chemistry, and Department of Biological Chemistry, University of Michigan, Ann Arbor, Michigan 48109-0606

Received November 1, 2001

ABSTRACT: The heme domain ($iNOS_{heme}$) of inducible nitric oxide synthase (iNOS) was expressed in *Escherichia coli* and purified to homogeneity. Characterization of the expressed $iNOS_{heme}$ shows it to behave in all respects like full-length iNOS. $iNOS_{heme}$ is isolated without bound pterin but can be readily reconstituted with (6*R*)-5,6,7,8-tetrahydro-L-biopterin (H_4B) or other pterins. The reactivity of pterin-bound and pterin-free $iNOS_{heme}$ was examined, using sodium dithionite as the reductant. H_4B-bound $iNOS_{heme}$ catalyzes both steps of the NOS reaction, hydroxylating arginine to N^G-hydroxy-L-arginine (NHA) and oxidizing NHA to citrulline and •NO. Maximal product formation (0.93 ± 0.12 equiv of NHA from arginine and 0.83 ± 0.08 equiv of citrulline from NHA) requires the addition of 2 to 2.5 electron equiv. Full reduction of H_4B-bound $iNOS_{heme}$ with dithionite also requires 2 to 2.5 electron equiv. These data together demonstrate that fully reduced H_4B-bound $iNOS_{heme}$ is able to catalyze the formation of 1 equiv of product in the absence of electrons from dithionite. Arginine hydroxylation requires the presence of a bound, redox-active tetrahydropterin; pterin-free $iNOS_{heme}$ or $iNOS_{heme}$ reconstituted with a redox-inactive analogue, 6(*R*,*S*)-methyl-5-deaza-5,6,7,8-tetrahydropterin, did not form NHA under these conditions. H_4B has an integral role in NHA oxidation as well. Pterin-free $iNOS_{heme}$ oxidizes NHA to citrulline, N^δ-cyanoornithine, an unidentified amino acid, and NO^-. Maximal product formation (0.75 ± 0.01 equiv of amino acid products) requires the addition of 2 to 2.5 electron equiv, but reduction of pterin-free $iNOS_{heme}$ requires only 1 to 1.5 electron equiv, indicating that both electrons for the oxidation of NHA by pterin-free $iNOS_{heme}$ are derived from dithionite. These data provide strong evidence that H_4B is involved in electron transfer in NOS catalysis.

The biosynthesis of •NO is catalyzed by the enzyme nitric oxide synthase (NOS,[1] EC 1.14.13.39) in a reaction that also forms citrulline from the amino acid L-arginine (for reviews, see refs *1*−*3*). In this five-electron oxidation, •NO is derived from one of the terminal guanidino nitrogens of arginine. The reaction proceeds in two steps, both of which require NADPH and O_2 as cosubstrates. The first step of the reaction is the hydroxylation of arginine, forming N^G-hydroxy-L-arginine (NHA) as an intermediate (*4*−*6*). NHA is further oxidized by three electrons in the second step to form citrulline and •NO. Three isoforms of NOS have been characterized: a particulate, constitutive enzyme from vascular endothelium (eNOS), a soluble, constitutive enzyme from neuronal cells (nNOS), and an inducible enzyme, best characterized from murine macrophages (iNOS) (*7*). All of the isoforms are homodimeric and bind an equivalent each of FAD, FMN (*8*−*10*), and protoporphyrin IX heme (*11*−*13*) per subunit. Full activity also requires one bound H_4B per monomer (*10*, *14*, *15*).

The roles of the enzyme-bound heme and H_4B in the reaction mechanism are not fully understood. CO inhibition studies have suggested a catalytic role for the heme in both steps of the NOS reaction (*16*, *11*). Further evidence for the involvement of the heme in NHA oxidation comes from NOS reactions where hydrogen peroxide is substituted for NADPH and O_2 (peroxide-shunt reactions). The products of the peroxide-shunt reactions are consistent with a heme ferric-peroxide nucleophile as an intermediate in the NADPH-dependent oxidation of NHA (*17*, *18*). A model for the enzymatic oxidation of NHA to citrulline and •NO, using an Fe^{III} porphyrin and O_2, has also been reported (*19*). The role of the heme in the hydroxylation of arginine has been less clear. Crystal structures of several NOS heme domains

† This research was supported by Howard Hughes Medical Institute and NIH Grant CA 50414. A.R.H. was supported by NIH Grant T32-GM07767, a Regents' Fellowship from the University of Michigan, and an American Foundation for Pharmaceutical Education Fellowship.

* To whom correspondence should be addressed at University of California, Berkeley, Department of Chemistry, 211 Lewis Hall, Berkeley, CA 94720-1460. Phone: (510) 643−9325; Fax: (510) 643−9388; E-mail: marletta@cchem.berkeley.edu.

‡ Department of Medicinal Chemistry, University of Michigan.

§ Howard Hughes Medical Institute, University of Michigan.

|| Department of Biological Chemistry, University of Michigan.

[1] Abbreviations: NOS, nitric oxide synthase; eNOS, endothelial NOS; nNOS, neuronal NOS; iNOS, inducible NOS; $iNOS_{heme}$, heme domain of inducible NOS; NHA, N^G-hydroxy-L-arginine; H_4B, (6*R*)-5,6,7,8-tetrahydro-L-biopterin; 7,8-H_2B, (6*R*)-7,8-dihydro-L-biopterin; MPH_4, 6(*R*,*S*)-methyl-5,6,7,8-tetrahydropterin; $DZPH_4$, 6(*R*,*S*)-methyl-5-deaza-5,6,7,8-tetrahydropterin; DTT, dithiothreitol; CN-orn, N^δ-cyanoornithine; HEPES, 4-(2-hydroxyethyl)-1-piperazineethane sulfonic acid; Tris-HCl, Tris[hydroxymethyl]aminomethane hydrochloride; IPTG, isopropyl-β-D-thiogalactopyranoside; PVDF, polyvinylidine fluoride; PCA, protocatechuic acid; PCD, protocatechuate 3,4-dioxygenase; Ni−NTA, nickel−nitrilotriacetic acid agarose; BSA, bovine serum albumin; NDA, 2,3-naphthalene dicarboxaldehyde; EDTA, ethylenediamine-*N*,*N*,*N*′,*N*′-tetraacetic acid; TFA, trifluoroacetic acid; EPR, electron paramagnetic resonance spectroscopy; PCR, polymerase chain reaction; MALDI, matrix-assisted laser desorption/ionization; HPLC, high-performance liquid chromatography; SDS−PAGE, sodium dodecyl sulfate−polyacrylamide gel electrophoresis; ICP/MS, inductively coupled plasma/mass spectrometry.

10.1021/bi012002h CCC: $22.00
Published on Web 02/12/2002

have been obtained (*20*−*23*), and this structural information supports the involvement of a heme-based oxidant in both steps of the NOS reaction. Arginine binds in the active site such that one of the terminal guanidino nitrogens is positioned to undergo hydroxylation by the heme; this nitrogen lies immediately above the plane of the porphyrin ring and is 3.8 Å away from the heme iron. The heme-based oxidant in this step is probably a high valent iron-oxo species such as that proposed for P450-catalyzed hydroxylations. NHA also binds adjacent to the heme iron (*24*−*26*), consistent with heme-dependent catalysis in the oxidation of NHA.

A direct role for H_4B in catalysis has been suggested since it was discovered that this redox cofactor is required for NOS activity (*27*, *28*, *14*). However, the nature of the involvement of H_4B in the NOS reaction has been obscured by observations that H_4B affects the stability of the NOS active site and its overall structure. The binding of H_4B to NOS has been shown to influence enzyme dimerization (*29*−*31*), binding affinity for substrate (*32*, *33*), heme spin state equilibrium (*34*, *35*), and heme midpoint potential (*36*). All of these observed effects can be understood by examining the crystal structures of H_4B-bound NOS (*20*−*23*). The structural data show that H_4B binds in close proximity to the heme cofactor and interacts with one of the heme propionate side-chains, providing a potential explanation for the effect of pterin on the spin state and redox potential of the heme. Similarly, the cooperativity of pterin and substrate binding is probably mediated by interactions of both molecules with the heme propionate. Finally, the pterin-binding site is located near the NOS dimer interface, and the bound pterin interacts with amino acids from both subunits. Although the pterin cofactor stabilizes the NOS structure, the effect of H_4B on catalysis is not completely explained by these structural effects. Several papers have described the reactivity of NOS in the presence of 4-aminotetrahydrobiopterin (*37*−*39*). This pterin binds with high affinity to NOS, effects a complete spin-state conversion of the heme, and stabilizes the NOS dimer, but is unable to support NOS catalysis. In fact, structures obtained with bound 4-amino-H_4B or the inactive 7,8-H_2B are indistinguishable from those with H_4B (*26*).

Recent proposals for the involvement of H_4B in the NOS reaction have focused on a role for this cofactor in electron transfer. These proposals were based on differences in the spectral decay of the ferrous-dioxygen complex of nNOS in the presence and absence of H_4B (*40*) and on the unique structural features of the pterin-binding site (*21*). Both papers speculated that a pterin radical might form in the NOS reaction. Direct evidence for a pterin radical ($H_3B\bullet$) in reactions of reduced $iNOS_{heme}$ with oxygen has been obtained by rapid freeze-quench EPR (*41*). The pterin radical probably arises from a one-electron reduction of the ferrous−dioxygen complex of $iNOS_{heme}$ by H_4B. $H_3B\bullet$ accumulates to 80% of the total $iNOS_{heme}$ concentration in the presence of arginine, and NHA is formed in this reaction, suggesting that H_4B is involved in electron transfer in the hydroxylation of arginine. In the presence of NHA, $H_3B\bullet$ only accumulates to 2.8% of the total $iNOS_{heme}$ concentration, and citrulline is formed. This small amount of $H_3B\bullet$ observed indicates either that $H_3B\bullet$ is not formed in the presence of NHA, or that it reacts rapidly in a subsequent step of the NHA reaction. These data support an integral and novel role for the pterin cofactor in NOS catalysis.

In this paper, we have used $iNOS_{heme}$ to study the mechanism of both steps of the NOS reaction. We have characterized the heterologously expressed $iNOS_{heme}$ and show it to behave in all respects like full-length iNOS. Because *Escherichia coli* have no endogenous H_4B, $iNOS_{heme}$ can be isolated without any bound pterin and subsequently reconstituted with H_4B or other pterins. Both pterin-bound and pterin-free forms of $iNOS_{heme}$ were used in these studies to investigate the role of H_4B in the enzyme reaction. In the absence of the reductase domain and its bound flavin cofactors, $iNOS_{heme}$ cannot accept electrons from NADPH. Although $iNOS_{heme}$ is thus dependent on an alternate reductant for catalysis, tighter control over the number of electrons delivered to the active site can be achieved. The ability of $iNOS_{heme}$ to hydroxylate arginine and to oxidize NHA was examined, using sodium dithionite as the reductant. The dependence of these reactions on exogenous electrons and the effect of pterin on the reaction products are reported. These results provide additional support for the involvement of H_4B in electron transfer in both steps of the NOS reaction.

EXPERIMENTAL PROCEDURES

Materials and General Methods. Escherichia coli JM109 competent cells and T4 DNA ligase were purchased from Promega. *E. coli* DH5α competent cells, DNA ladders (123 bp and 1 kb), and Terrific Broth (TB) were purchased from Life Technologies. Bacto-tryptone, yeast extract, and bacto-agar were obtained from Difco Laboratories. All restriction enzymes were from New England Biolabs. Alkaline phosphatase (from calf intestine), ampicillin, IPTG, and the Expand High Fidelity PCR kit were from Roche Molecular Biochemicals. The QIAfilter Plasmid kit and QIAquick Gel Extraction kit were purchased from QIAGEN. iNOS cDNA (GenBank accession #92649) in pBluescript II KS was a gift from Dr. Solomon H. Snyder (Johns Hopkins University). The pCWori plasmid (ampicillin resistance, tac-tac promoter) was a gift from Dr. Michael R. Waterman (Vanderbilt University), and the pKEN2 plasmid (ampicillin resistance, srp and T7 promoters) was a gift from Dr. Gregory L. Verdine (Harvard University). DNA oligomers were synthesized by the University of Michigan Biomedical Research Core Facilities. Precast 10 and 10−20% Tris−glycine gels and Mark 12 molecular weight standards were from Invitrogen. Coomassie Blue R-250, PVDF membrane, and Bradford protein reagent dye were purchased from Bio-Rad. Reaction vials and silicone/Teflon septa were obtained from Pierce Chemical Co. Gastight syringes were purchased from Hamilton Co. Centrifugal filtration units (Ultrafree-15 Biomax-30K NMWL and Ultrafree-0.5 Biomax-10K NMWL membrane) were from Millipore. NHA was purchased either from Alexis Corp. or Cayman Chemical Co. (Ann Arbor, MI) and was found to contain less than 2% citrulline contamination as analyzed by HPLC. PCA and PCD were gifts from Dr. David P. Ballou (University of Michigan). Sodium dithionite was purchased from Aldrich; solutions were prepared in 100 mM HEPES (pH 7.5) in an anaerobic chamber (Coy Laboratory Products) and were standardized against potassium ferricyanide before use (*42*). All other reagents were purchased from Sigma.

Construction of iNOS$_{heme}$ Expression Vector. An initial iNOS$_{heme}$ construct in the pKEN2 plasmid (MKR-iNOS$_{heme}$) was previously described (*43*). This heme domain construct includes amino acids 1−490 of the iNOS sequence and also contains a C-terminal hexahistidine tag. SDS−PAGE analysis of iNOS$_{heme}$ expressed from the MKR-iNOS$_{heme}$ vector showed a doublet of bands, which were confirmed by N-terminal sequencing (A. R. Hurshman and M. A. Marletta, unpublished results) to arise from an alternate start site at amino acid position 28 (GTG, coding for Val, but able to serve as an initiation codon). Further PCR was carried out to change this codon from GTG to GTT, still coding for valine, but no longer an alternate start site. This strategy was carried out using two mutagenic primers and the overlap extension method. The four primers used were as follows: primer 1, sense outer primer TAATACGACTCACTATAGGG; primer 2, sense mutagenic primer ACAACAACGT**T**AAGAAAACCC; primer 3, antisense mutagenic primer GGGTTTTCTT**A**ACGTTGTTGT; primer 4, antisense outer primer TCAAAGACCTGCAGGTTGGAC. In the first round of PCR, MKR-iNOS$_{heme}$ was amplified with primers 1 and 3 to yield a 241-bp fragment, and iNOS cDNA in pBluescript II KS was amplified with primers 2 and 4 to yield a 547-bp fragment. A second round of PCR, using the 241-bp and 547-bp fragments as the template and primers 1 and 4, gave a fragment of the expected length (767 bp). The 767-bp PCR product was digested with *Bam*HI and ligated into the *Bam*HI sites of MKR-iNOS$_{heme}$ to make pKEN2iNOS$_{heme}$. The expression vector pCWiNOS$_{heme}$ was made by subcloning the entire iNOS$_{heme}$ gene (1.5-kb fragment from *Nde*I and *Hind*III digestion of pKEN2iNOS$_{heme}$) into the *Nde*I and *Hind*III sites of pCW. The *E. coli* strains JM109 and DH5α were used for all DNA manipulations. Purified plasmid DNA and PCR products were sequenced by the University of Michigan Biomedical Research Core Facilities to confirm the absence of mutations arising from PCR.

Expression of iNOS$_{heme}$. Optimal expression of iNOS$_{heme}$ was obtained in JM109 cells grown in Terrific Broth (47 g/L TB and 4 mL/L glycerol). Expression cultures (1.5 L of TB containing 50 μg/mL ampicillin) were inoculated (1:100) from an overnight culture of JM109−pCWiNOS$_{heme}$ and were grown at 37 °C to an A_{600} of ∼0.5. The cultures were then cooled to 25 °C, induced by the addition of IPTG (0.4 mM final concentration), and harvested by centrifugation (10 min at 15 900*g*) 21 h after induction.

Purification of iNOS$_{heme}$. Purification of iNOS$_{heme}$ was achieved in three steps, as previously described (*41*). Briefly, supernatant was prepared from fresh cell pellets, and iNOS$_{heme}$ was purified by metal affinity chromatography (Ni−NTA agarose from QIAGEN), followed by gel filtration on Superdex 200 (HiLoad 26/60 from Amersham Pharmacia Biotech) and finally by anion exchange (Q-HyperD, 10 μm column from Beckman). Fractions containing iNOS$_{heme}$ were red in color and were pooled after each step on the basis of the A_{280}/A_{428} (protein to heme) ratio. Following purification, iNOS$_{heme}$ was stored at −80 °C in 20 mM Tris-HCl (pH 8.0), with 2 mM imidazole and 300 mM NaCl (anion exchange elution buffer). Protein concentration was determined in one of two ways, depending on the experiment, and is shown as the concentration of iNOS$_{heme}$ monomer: (i) Protein concentrations used for calculating the stoichiometry of cofactor and metal binding, as well as the extinction coefficient at 280 nm, were determined by the Bradford protein assay with BSA as the standard. (ii) For all other experiments, iNOS$_{heme}$ concentrations were determined spectrophotometrically, using the heme Soret extinction coefficients reported below, and represent only the fraction of protein that has bound heme.

Amino Acid Sequencing. N-Terminal amino acid sequences were determined by Edman degradation by the University of Michigan Biomedical Research Core Facilities, using an Applied Biosystems sequenator. Purified iNOS$_{heme}$ was loaded on a 10% precast Tris−glycine gel, electrophoresed at 200 V for 75 min, and then transferred to a PVDF membrane by electroblotting at 200 mA for 1 h. The electroblot buffer was 10 mM CAPS (3-cyclohexylamino-1-propanesulfonic acid, pH 10.5), with 0.05% DTT and 15% methanol. The membrane was stained with Coomassie Blue R-250 to visualize the protein bands. The bands were excised, dried in microcentrifuge tubes, and submitted for analysis.

Subunit Molecular Weight Determination. The molecular weight of iNOS$_{heme}$ monomer was determined by MALDI mass spectrometry on a VESTEC-2000 instrument at the University of Michigan Biomedical Research Core Facilities.

Pterin Stock Solutions. H_4B and MPH_4 were purchased from Schircks Laboratories (Jona, Switzerland) and were prepared either in 100 mM HEPES (pH 7.5) containing 100 mM DTT or in an anaerobic chamber in 100 mM HEPES (pH 7.5) with no DTT. H_4B concentrations were determined spectrophotometrically in 100 mM HEPES (pH 8.0) from the absorbance at 297 nm, using the published extinction coefficient ($\epsilon_{297} = 8700\ M^{-1}\ cm^{-1}$; *44*). MPH_4 concentrations were similarly determined in 0.1 N HCl, recording the absorbance at 265 nm ($\epsilon_{265} = 14\ 380\ M^{-1}\ cm^{-1}$; *45*). $DZPH_4$ was synthesized as previously described (*14*, *46*) and was used as the monotrifluoroacetate salt. Stock solutions were prepared by dissolving 4−6 mg of $DZPH_4$ in 0.5 mL of 0.1 N NaOH, diluting to 4 mL with 200 mM HEPES (pH 7.4), and adjusting the pH to 7.4 with HCl. $DZPH_4$ concentrations were determined in 100 mM HEPES (pH 8.0) from the absorbance at 279 nm ($\epsilon_{279} = 15\ 500\ M^{-1}\ cm^{-1}$; *46*).

Preparation of H_4B-Bound iNOS$_{heme}$. Expressed in *E. coli*, iNOS$_{heme}$ contains no bound pterin, and the omission of H_4B in all purification steps results in a pterin-free iNOS$_{heme}$ preparation. Furthermore, all of the purification buffers contain at least 2 mM imidazole, so iNOS$_{heme}$ is purified as the imidazole complex (λ_{max} at 428 nm). Most of the experiments described here were carried out with H_4B-bound iNOS$_{heme}$, reconstituted as follows: iNOS$_{heme}$ (as purified, 50 μM) was incubated with 500 μM H_4B, 5 mM DTT, and 100 mM arginine for 1 h at 4 °C. The spectrum of iNOS$_{heme}$ following this incubation confirmed a complete conversion to high-spin heme (λ_{max} at 396 nm). H_4B-bound iNOS$_{heme}$ was concentrated to 0.1−1 mM and stored at −80 °C with 30% glycerol in aliquots of less than 300 μL. Preparations of H_4B-bound iNOS$_{heme}$ (<300 μL) were desalted immediately prior to use on Sephadex G25M (PD10 prepacked columns from Pharmacia Amersham Biotech) into 100 mM HEPES (pH 7.5). This desalting step removes imidazole, arginine, glycerol, DTT, and any H_4B that is not bound to iNOS$_{heme}$. iNOS$_{heme}$ was either diluted with 100 mM HEPES (pH 7.5) or concentrated in Ultrafree-0.5 devices to the desired concentration, depending on the experiment.

Preparation of Pterin-Free iNOS$_{heme}$. iNOS$_{heme}$ as purified (imidazole complex, no bound pterin) was concentrated to 0.1−1 mM and stored at −80 °C in aliquots of less than 300 μL. These samples were desalted (<300 μL applied to PD10 column equilibrated with 100 mM HEPES, pH 7.5) immediately prior to use to remove the bound imidazole. Pterin-free iNOS$_{heme}$ was either diluted or concentrated as above to the desired concentration.

Determination of Bound Cofactors. Unless otherwise specified, iNOS$_{heme}$ samples were desalted into 100 mM HEPES (pH 7.5) containing 100 μM arginine. The concentration of iNOS$_{heme}$ samples applied to the PD10 columns was 200−800 μM, to give a concentration after desalting in the range of 50−200 μM. Samples were subsequently diluted to obtain the concentration required for the various analyses.

Heme Content. Heme analysis was carried out by an HPLC method (adapted from ref *47*), using a Protein C_4 column (250 × 4.6 mm, 5 μm, Vydac) and a Beckman System Gold HPLC with a diode array detector. Samples (25 μL of 1−5 μM iNOS$_{heme}$) were applied to the column, which was equilibrated with 0.1% aqueous TFA (solvent A) and maintained at 40 °C. Elution conditions were 0−75% solvent B (0.1% TFA in acetonitrile) over 20 min (flow rate of 0.2 mL/min), followed by 75−100% solvent B over 2 min, 100% solvent B for 5 min, and then a return to 100% solvent A over the final 3 min. The retention time of heme (detected at 400 nm) was 23 min, and myoglobin standards (0.25−10 μM) were used to determine the heme content of iNOS$_{heme}$ samples.

Pterin Content. The pterin content of iNOS$_{heme}$ samples was determined by HPLC on a Nova-Pak C_{18} column (150 × 3.9 mm, 4 μm, Waters) equipped with an Alltima C_{18}-LL guard column (5 μm, Alltech), using a Hewlett-Packard 1090 series II HPLC with a diode array detector. Standards (4−100 μM) and protein samples (10−40 μM, with 1 mM arginine) contained 10 mM DTT and 0.8 M guanidine HCl and were prepared immediately prior to analysis to minimize pterin oxidation. The column was maintained at 40 °C, and the flow rate was 0.5 mL/min. Solvent A consisted of 50 mM sodium acetate, 5 mM citric acid, and 50 μM EDTA (pH 6.0) (*48*, *49*), and the column was equilibrated with 100% solvent A for 3 min prior to each injection (10 μL of sample). Elution conditions were 0−20% solvent B (methanol) over 9 min, followed by 20−80% solvent B over 3 min, a linear increase to 100% solvent B over 0.5 min, and then a return to 100% solvent A over the final 0.5 min. Pterin species were detected at 297 nm (λ_{max} for H_4B) and 280 nm (λ_{max} for 7,8-H_2B). Retention times under these conditions are as follows: H_4B, 4.0 min; 7,8-H_2B, 4.8 min; oxidized DTT, 9.7 min. 7,8-H_2B was not detected in either the standards or protein samples; H_4B standards were used to quantify the pterin in each iNOS$_{heme}$ sample.

Metal Analysis. ICP/MS (Plasmaspec III, Leeman Labs, Hudson, NH) analysis of iNOS$_{heme}$ samples was carried out by Dr. Ted J. Huston (Department of Geological Sciences, University of Michigan, Ann Arbor). All samples were diluted into metal-free buffer (to give a metal concentration ~1 μM) and were analyzed for iron, nickel, copper, and zinc. Buffer controls (PD10 fraction immediately preceding that containing protein) were also analyzed for metal content.

Quantitative Amino Acid Analysis. Samples for amino acid analysis were prepared as described above, except that the desalting step did not include arginine, which would interfere with the analysis. Amino acid analysis (QAA) was carried out by the University of Michigan Biomedical Research Core Facilities. The Bradford correction factor for iNOS$_{heme}$ was determined by comparison of the protein concentration obtained by quantitative amino acid analysis with that obtained by the Bradford protein assay. The protein concentration of iNOS$_{heme}$ samples was determined by the Bradford method both prior to sample submission and following analysis (remaining sample was recovered from the Core); in all cases, the protein concentration determined after amino acid analysis was within 5% of that determined beforehand.

Determination of Extinction Coefficients. The extinction coefficients for arginine-bound (100 μM arginine present) ferric iNOS$_{heme}$ were determined by comparison of the absorbance spectrum of each sample (1−5 μM) with the heme concentration determined by the HPLC method described above. The extinction coefficient for the protein peak of ferric iNOS$_{heme}$ was similarly determined by comparison of the absorbance at 280 nm with the protein concentration determined by the Bradford protein assay. The extinction coefficients for imidazole-bound ferric iNOS$_{heme}$ were determined from the spectrum recorded in the presence of 1 mM imidazole. For reduced forms of iNOS$_{heme}$, the spectrum of the arginine-bound ferric iNOS$_{heme}$ was recorded prior to reduction of the sample. Samples were reduced with dithionite under an atmosphere of either argon (99.9999% pure, <0.5 ppm O_2, Matheson Gas Products) or CO (99.99% pure, <0.5 ppm O_2, Matheson) in an anaerobic cuvette sealed with a rubber septum. Extinction coefficients were calculated for the ferrous-deoxy and ferrous−CO species by comparison of each reduced spectrum to the corresponding oxidized spectrum, using the ϵ_{396} determined above to calculate the heme concentration of each sample.

K_d Titrations. H_4B-bound iNOS$_{heme}$ (400 μL of 0.5−1 μM) was titrated with arginine or NHA to spectrophotometrically determine the binding affinity (spectral K_d) for each substrate. Spectra were corrected for dilution after each addition; the total change in volume over the course of each titration was less than 5%. The absorbance changes in the difference spectra ($\Delta\Delta Abs = \Delta Abs_{max} - \Delta Abs_{min}$) were plotted as a function of substrate concentration, and K_d was determined by fitting the data by a nonlinear least-squares fit to the saturation binding equation: $\Delta\Delta Abs = (\Delta\Delta Abs_{max} \times [substrate])/(K_d + [substrate])$ (KaleidaGraph 3.0.8, Abelbeck Software). Similar titrations were carried out to determine K_d for binding of $DZPH_4$ to pterin-free iNOS$_{heme}$ (1−2.5 μM).

Analytical Gel Filtration. Samples (50 μL of 2−20 μM) of iNOS$_{heme}$ were applied to a TosoHaas QC−PAK TSK 300GL column (150 × 8 mm, 5 μm) equilibrated with 100 mM HEPES (pH 7.5) containing 200 mM NaCl. The flow rate was 0.9 mL/min. Standards (1 mg/mL) used for molecular weight determinations were thyroglobulin (669 kDa), apoferritin (443 kDa), alcohol dehydrogenase (150 kDa), bovine serum albumin (66 kDa), egg albumin (45 kDa), and carbonic anhydrase (29 kDa). The apparent native molecular weight of iNOS$_{heme}$ was calculated from the standard curve of the natural logarithm of the molecular weight of the standards vs retention time.

Native Gel Electrophoresis. Native PAGE was also used to determine the oligomeric state of iNOS$_{heme}$. Samples (10−

20 μg) were loaded on 10−20% precast Tris−glycine gels and were electrophoresed for 2 h (4 °C, 200 V) under nondenaturing, nonreducing conditions.

Dithionite-Dependent Enzyme Reactions. Following desalting, $iNOS_{heme}$ (either H_4B-bound or pterin-free) was concentrated to 80 μM. $iNOS_{heme}$ samples were made anaerobic in sealed 3-mL reaction vials by 10 cycles of alternate evacuation and purging with purified argon, using an anaerobic gas-train. Reactions were carried out in sealed 0.3-mL reaction vials. $iNOS_{heme}$ (50 μL) was transferred to each vial in an anaerobic chamber. Reactions contained 1 mM of either arginine or NHA, depending on the experiment. Sodium dithionite was added to reduce each sample; the concentration of dithionite added varied from 10 to 240 μM (to provide 0.25−6 electrons per $iNOS_{heme}$). Reactions were initiated by the addition of 50 μL of oxygenated buffer (100 mM HEPES, pH 7.5, containing 1 mM of the appropriate substrate and 100 μM phenylalanine, and oxygenated by purging with pure oxygen gas for 30 min on ice) in a gastight syringe to each reaction vial. After mixing of the samples, reactions contained 40 μM $iNOS_{heme}$, 1 mM substrate, 5−120 μM dithionite, 50 μM phenylalanine, and 1.1 mM O_2 in 100 mM HEPES (pH 7.5) in a total volume of 100 μL. Reaction mixtures remained at 25 °C for 1 h prior to analysis to ensure full conversion of the inorganic product of the reaction to NO_2^-/NO_3^-.

Anaerobic Pterin Incubations. To examine the role of pterin in $iNOS_{heme}$, some dithionite reactions were carried out with pterin-free $iNOS_{heme}$ incubated with various pterins under anaerobic conditions. Pterin-free $iNOS_{heme}$ (80−100 μM) was desalted, concentrated, and made anaerobic in 3-mL reaction vials, as described above. Experiments were carried out in one of two ways: (i) Anaerobic pterin-free $iNOS_{heme}$ (200 μL of 82 μM) was incubated for 2 h on ice with buffer alone, 200 μM H_4B, 500 μM $DZPH_4$, or 500 μM MPH_4 in 250 μL total volume. Incubations also contained 1 mM of arginine or NHA to facilitate binding of the pterin to $iNOS_{heme}$. After 2 h, aliquots of the incubation mixture (40 μL of 66 μM $iNOS_{heme}$) were transferred to 0.3-mL reaction vials, and these samples were reduced with 16.5−132 μM dithionite (0.5−4 electrons per $iNOS_{heme}$). Reactions were initiated with oxygenated buffer (40 μL) and analyzed as described above. (ii) Anaerobic pterin-free $iNOS_{heme}$ (40 μL of 100 μM, with 1 mM arginine) was transferred to each 0.3-mL reaction vial and incubated for 2 h with buffer alone, H_4B (20−340 μM), $DZPH_4$ (50−1000 μM), or MPH_4 (50−1000 μM) in 50 μL total volume. Samples (80 μM $iNOS_{heme}$) were reduced with 80 μM dithionite (2 electrons per $iNOS_{heme}$), and reactions were initiated and analyzed as described above.

Quantitation of Amino Acid Products. The amino acid products of the enzyme reactions described above were analyzed by HPLC. Amino acids were derivatized with NDA (*50*) and then separated by reverse-phase HPLC on a Nova-Pak C_{18} column (150 × 3.9 mm, 4 μm, Waters) equipped with an Alltima C_{18}-LL guard column (5 μm, Alltech), using a Hewlett-Packard 1090 series II HPLC with a diode array detector. Derivatization conditions were as follows: 21 μL of sample, 9 μL of 50 mM NaCN in 0.1 M potassium borate (pH 9.5), and 3 μL of 10 mM NDA in methanol were reacted for 15 min immediately prior to injection onto the column. The column was maintained at 40 °C, and the flow rate was 0.5 mL/min. NHA and citrulline standards were used to quantify the reaction products, with phenylalanine as an internal standard. Two different separation methods were used, depending on the substrate of the reaction. In both cases, solvent A consisted of 5 mM ammonium acetate (pH 6.0) to which 20% methanol (v/v) had been added.

(A) Arginine Reactions. The column was equilibrated with 20% solvent B (acetonitrile) for 3 min prior to each injection (25 μL of derivatized sample). Elution conditions were 20% solvent B for 4 min, followed by a linear gradient of 20−65% solvent B over 4.5 min, 65−100% solvent B over 0.5 min, 100% solvent B for 3 min, and a return to the initial conditions (20% solvent B) over the final 0.5 min. Retention times: citrulline, 3.1 min; NHA, 5.9 min; arginine, 7.2 min; phenylalanine, 8.5 min.

(B) NHA Reactions. Arginine and NHA are well resolved by the above method; however, it cannot be used for reactions where NHA is the substrate, because citrulline and CN-orn coelute under these conditions. The following method was used instead for NHA reactions, where solvent B is methanol. The column was equilibrated with 100% solvent A for 3 min prior to each injection (25 μL of derivatized sample). Elution conditions were 0−35% solvent B over 4 min, 35−50% solvent B over 3 min, followed by a linear increase to 100% solvent B over 2 min, 100% solvent B for 3 min, and a return to 100% solvent A over the next 0.5 min. Retention times: citrulline, 7.1 min; CN-orn, 7.9 min; NHA, 9.0 min; phenylalanine, 10.1 min.

Quantitation of Nitrite and Nitrate. Nitrite/nitrate formed in the enzyme reactions was quantified using the NO_2^-/NO_3^- colorimetric assay kit from Cayman Chemical Co. (Ann Arbor, MI). Briefly, NO_3^- was enzymatically reduced to NO_2^-, and then total NO_2^- plus NO_3^- was determined by the reaction of NO_2^- with the Griess reagent (*51*). Assays were carried out in 96-well plates, and product was quantified by comparison with authentic standards.

•NO Detection. Some dithionite-dependent reaction mixtures were analyzed for •NO formation. A Sievers model 270 •NO chemiluminescence detector (Boulder, CO) was used to detect •NO, as previously described (*35*). For these reactions, 100 μL of headspace gas was drawn in a gastight syringe and injected into the manifold of the •NO analyzer, which contained 5 mL of 1 M NaOH with 0.2% antifoam SO-25. The headspace was sampled within 1 min of the addition of oxygenated buffer to the sealed reaction vials. The detection limit of the instrument reported by the manufacturer is ∼10 fmol of •NO.

Dithionite Titrations. Pterin-free and H_4B-bound $iNOS_{heme}$ were titrated with dithionite to determine the number of reducing equivalents necessary to fully reduce the enzyme. Titrations were carried out in the absence of substrate or in the presence of 1 mM arginine or NHA. $iNOS_{heme}$ samples (1−1.5 mL of 20−25 μM) were made anaerobic in an anaerobic cuvette by 10 cycles of alternate evacuation and purging with purified argon, using an anaerobic gas-train. PCA (250 μM) and PCD (0.8 units/mL; 1 unit is the amount of enzyme that catalyzes the disappearance of 1 μmol of substrate per min at 25 °C in 100 mM HEPES, pH 7.5) were added to consume any residual oxygen; the PCD was added to the sidearm of the cuvette and mixed in after the final vacuum/purge cycle. A solution of sodium dithionite was prepared, standardized against potassium ferricyanide, and

Table 1: Cofactor and Metal Binding to H_4B-Bound $iNOS_{heme}$[a]

analyte	stoichiometry (per $iNOS_{heme}$ monomer)	
heme[b]	0.85 ± 0.05	(n = 8)
iron[c]	0.84 ± 0.09	(n = 8)
nickel	0.03 ± 0.01	(n = 8)
copper	0.006 ± 0.001	(n = 8)
zinc	0.23 ± 0.04	(n = 8)
H_4B[d]	0.86 ± 0.08	(n = 7)

[a] Protein concentration was determined by the Bradford protein assay. The stoichiometry in each case represents the mean of 7 or 8 different preparations of $iNOS_{heme}$, and the standard deviation for each sample relative to the mean is shown. [b] Heme content was determined from duplicate measurements of two dilutions of each sample. [c] Metal content for each sample was determined in triplicate. Buffer controls contained at most the metal concentration indicated, expressed as a percentage of the concentration of metal in the protein samples: iron, 0.04−0.15%; nickel, 0.6−3.4%; copper, 6−11%; zinc, 0.2−0.6%. [d] H_4B content for each sample was determined at least in duplicate. No H_4B (or other pterin) was detected in pterin-free $iNOS_{heme}$ samples, even at 100 μM concentration of $iNOS_{heme}$. With a lower limit of detection for this method of less than 0.1 μM, the maximal stoichiometry of pterin bound to pterin-free $iNOS_{heme}$ is 0.001.

transferred to a titrating syringe. The titrating syringe was attached to the top of the anaerobic cuvette through a ground-glass joint during the last purge cycle, while maintaining the cuvette under positive pressure. Dithionite was added to $iNOS_{heme}$ in substoichiometric increments, and UV−visible spectra were recorded after each dithionite addition. The extent of heme reduction at each dithionite concentration was determined by deconvoluting the spectra into their oxidized and reduced components. Dithionite was added until the heme was completely reduced (λ_{max} at 414 nm); further additions of dithionite resulted in an increase in absorbance at 314 nm, indicating the presence of excess dithionite, with no additional changes to the heme Soret. Each spectrum was corrected for dilution; the total change in volume over the course of each titration was less than 3%. All dithionite titration experiments were done at 25 °C.

UV−Visible Absorbance Spectroscopy. UV−visible spectra were recorded on a Cary 3E spectrophotometer (Varian) equipped with a Neslab RTE−111 circulating water bath. Unless otherwise specified, all spectral experiments were carried out at 15 °C.

RESULTS

Purification of $iNOS_{heme}$. $iNOS_{heme}$ was expressed in *E. coli* with a C-terminal hexahistidine tag, and thus the first step in the purification is metal affinity chromatography, using Ni−NTA agarose. Although this step is often sufficient for purification of His-tagged proteins, the purity of $iNOS_{heme}$ following this step is only 70−75%. Purification of $iNOS_{heme}$ was accomplished in two subsequent steps, using gel filtration and anion exchange chromatography. This purification method yields 25−30 mg of $iNOS_{heme}$ from 9 L of *E. coli* cell culture, with an A_{280}/A_{428} ratio of 1.3−1.35 and judged to be greater than 95% pure by SDS−PAGE with Coomassie staining.

The purification is carried out in the absence of H_4B. Since $iNOS_{heme}$ expressed in *E. coli* contains no bound pterin, the omission of H_4B in all purification steps results in a pterin-free $iNOS_{heme}$ preparation. Furthermore, imidazole (2 mM) is included throughout the purification because early observations indicated that the pterin-free $iNOS_{heme}$ is more stable in the presence of imidazole (A. R. Hurshman and M. A. Marletta, unpublished results). Thus, $iNOS_{heme}$ is purified as the imidazole complex (λ_{max} at 428 nm; see Table 2) and reconstituted with H_4B as needed after purification.

N-Terminal Heterogeneity of $iNOS_{heme}$. The subunit molecular mass of $iNOS_{heme}$ is calculated from the sequence to be 56.9 kDa (for intact $iNOS_{heme}$ without the N-terminal methionine). As purified, $iNOS_{heme}$ preparations migrate on SDS−PAGE as a multiplet of bands (data not shown). The calculated molecular weight (using Mark12 protein standards) for these bands is 57 kDa (band 1), 54 kDa (band 2), and 52 kDa (band 3). All of the bands react with iNOS polyclonal antibodies (not shown). N-terminal sequencing of the individual bands indicates that the heterogeneity on SDS−PAGE is due to differences at the N-terminus. Band 1 contains a mixture of intact $iNOS_{heme}$ (no N-terminal methionine, Δ1, 56.9 kDa), Δ6 (56.4 kDa), and Δ13 (55.5 kDa) fragments. Band 2 corresponds to a Δ34 fragment (53.0 kDa), and band 3 corresponds to a Δ54 fragment (50.9 kDa). MALDI mass spectrometry of purified $iNOS_{heme}$ shows two broad peaks: one corresponding to molecular masses in the range 55.0−57.5 kDa (band 1) and the other corresponding to 52.2−53.5 kDa (band 2). The MALDI data indicate that the predominant form of the purified $iNOS_{heme}$ is the Δ13 fragment. These fragments likely arise from proteolysis, despite the presence of a cocktail of protease inhibitors in the initial steps of the purification.

The same fragments and a similar distribution of $iNOS_{heme}$ forms have previously been reported (*52*). The expression of a truncated iNOS heme domain, lacking amino acids 1−65 (Δ65 $iNOS_{ox}$), was also reported in that same paper (*52*). This truncated mutant maintains high-affinity binding of both

Table 2: Spectral Characterization of $iNOS_{heme}$[a]

	δ	Soret	α/β	por → Fe CT[b]
ferric species				
pterin-free	∼360	∼421	540, 576	650
H_4B-bound		∼400	514, 546[c]	650
arginine		396 (85.1)	514 (13.6), 546[c] (10.9)	650 (4.9)
NHA		396	514, 546[c]	650
imidazole	363 (33.2)	428 (92.3)	549 (13.3), 582[c] (8.1)	730 (2.0)
ferrous species				
ferrous-deoxy		414 (71.1), 450[c] (32.6)	556 (11.5)	
ferrous−CO	381[d] (32.2)	420[c] (34.0), 445 (105.4)	554 (10.9), 590[c] (6.5)	

[a] The absorbance maxima (λ_{max}) for each species are shown, with the calculated extinction coefficients (ϵ, in mM^{-1} cm^{-1}) in parentheses. The extinction coefficients are averages of several determinations (n = 16 for arginine-bound and n = 6 for all others); the standard deviation is less than ± 5% in all cases. [b] Porphyrin-to-iron charge-transfer band. [c] Shoulder. [d] Indicated wavelength is not the peak; actual peak position could not be determined because of the presence of dithionite.

arginine and the pterin cofactor. Additionally, this fragment (residues 65−498 of iNOS) was used in crystallographic studies to determine the structure of H_4B-bound $iNOS_{heme}$ (*20*). On the basis of these observations, the N-terminus of the iNOS sequence (amino acids 1−75) appears not to be essential for a native active site, consistent with sequence alignments that show this to be a region of low homology among the NOS isoforms.

The gel filtration step of the purification described here partially resolves the $iNOS_{heme}$ bands, and thus $iNOS_{heme}$ preparations can be enriched in the higher molecular weight bands by careful pooling of the fractions from the Superdex 200 column. $iNOS_{heme}$ used in these studies ran on SDS−PAGE as a mixture of the 57 kDa (85−90%) and 54 kDa (10−15%) bands, with no detectable (<5%) 52 kDa band. The observed N-terminal heterogeneity does not appear to result in any functional heterogeneity in these $iNOS_{heme}$ preparations.

Stoichiometry of Cofactor Binding. The ability of H_4B-reconstituted $iNOS_{heme}$ to bind the cofactors necessary for catalysis was examined (Table 1).

(A) Heme and Metal Content. The heme content in all the samples is high (0.85 per monomer). The iron content determined by ICP/MS is 0.84 per monomer, in excellent agreement with the heme stoichiometry, indicating that there is no non-heme iron in these $iNOS_{heme}$ samples. The only other metal species present in significant amount is zinc, bound with a stoichiometry of 0.23 per monomer. The presence of zinc is expected on the basis of several crystal structures, which show a zinc tetrathiolate center at the dimer interface of both endothelial and inducible NOS heme domains (*21*−*23*). The exact role of the zinc in NOS is not known, but it appears to be structural rather than catalytic (*53*, *54*). The stoichiometry reported here is lower (about half) than the 0.5 per monomer predicted by the crystallographic data; this low zinc content has no obvious adverse effect on these $iNOS_{heme}$ preparations. A small amount of nickel is also detected (0.03 per monomer), probably a result of nickel binding to the His-tag during purification on the nickel column.

(B) Pterin Content. The stoichiometry of bound H_4B is 0.86 per monomer, equivalent to the heme stoichiometry. Previous reports indicate that the pterin cofactor does not bind to heme-free NOS (*29*, *55*−*57*). We assume on the basis of these observations that the fraction of $iNOS_{heme}$ that has bound heme is able to bind the pterin cofactor, and the remaining 15% that does not bind pterin probably represents heme-free $iNOS_{heme}$. Pterin-free preparations were also analyzed for H_4B content. No H_4B (or other pterin) was detected in these samples, even at 100 μM concentration of $iNOS_{heme}$ (data not shown). With a lower limit of detection for the HPLC method of less than 0.1 μM, the stoichiometry of H_4B bound to pterin-free $iNOS_{heme}$ is at most 0.001 per monomer.

(C) Bradford Correction Factor. The stoichiometries reported here were calculated using the protein concentrations determined by the Bradford protein assay. Quantitative amino acid analysis (QAA) was used to determine a Bradford correction factor (protein concentration determined by Bradford divided by protein concentration determined by QAA) for $iNOS_{heme}$. QAA did not detect any tryptophan (12 present in the $iNOS_{heme}$ sequence) or cysteine (10 in $iNOS_{heme}$) residues, so these amino acids were excluded from the analysis. The protein concentration by QAA was therefore determined by summing the picomole quantities of the individual amino acids and dividing this total by 473, the length of $iNOS_{heme}$ without the 12 tryptophans, 10 cysteines, and the N-terminal methionine. The concentration of $iNOS_{heme}$ determined by the two methods was then compared, and the Bradford correction factor was calculated to be 1.06 ± 0.11 ($n = 6$). This value indicates that the Bradford assay may result in a slight overestimation of the actual $iNOS_{heme}$ concentration. However, because the correction is small and the error of both methods is ∼10%, no Bradford correction was applied.

Spectral Characterization of $iNOS_{heme}$. The spectral features of various forms of $iNOS_{heme}$ are summarized in Table 2. In all cases, the observed spectra are indistinguishable from those of full-length iNOS, except for the absence of flavins in $iNOS_{heme}$.

(A) H_4B-Bound and Pterin-Free $iNOS_{heme}$. As is the case with full-length NOS (*34*, *35*), the presence of H_4B has a significant effect on the spectral properties of $iNOS_{heme}$. The spectra of both H_4B-bound and pterin-free $iNOS_{heme}$ show a mixture of high- and low-spin heme, but the relative amount of each depends on the presence of H_4B. H_4B-bound $iNOS_{heme}$ (λ_{max} of Soret ∼400 nm) is composed primarily (85−90%) of high-spin heme, with a small amount of low-spin heme. In contrast, pterin-free $iNOS_{heme}$ (λ_{max} ∼421 nm) is predominantly low-spin (probably ∼70%, but difficult to estimate because the spectrum of 100% low-spin has not been observed). Since these preparations are mixtures of heme spin states and the relative amount of high- and low-spin heme varies somewhat from preparation to preparation, extinction coefficients could not be accurately determined.

(B) Effect of Substrate and Imidazole. Addition of either arginine or NHA results in a low- to high-spin state conversion of the heme of $iNOS_{heme}$, analogous to spectral changes caused by substrate binding to other P450 enzymes. Upon substrate addition to H_4B-bound $iNOS_{heme}$, the Soret shifts to 396 nm, indicating a complete shift to high-spin heme. Both substrates also effect some spin-state conversion of the heme in pterin-free $iNOS_{heme}$, but to a much lesser extent. Full conversion to high-spin heme in this case requires the addition of H_4B. Extinction coefficients were only calculated for the arginine-bound ferric enzyme but are expected to be similar or identical for NHA-bound $iNOS_{heme}$. The extinction coefficient for the protein absorbance at 280 nm (not shown in Table 2) is $100\,600 \pm 4\,500$ M^{-1} cm^{-1} ($n = 8$). Imidazole binds to both H_4B-bound and pterin-free $iNOS_{heme}$. The spectrum of imidazole-bound $iNOS_{heme}$ (λ_{max} 428 nm) is indicative of a six-coordinate, low-spin complex, with one of the imidazole nitrogens coordinating the heme iron.

(C) Ferrous and Ferrous−CO $iNOS_{heme}$. All of the ferric forms of $iNOS_{heme}$ described above can be reduced by dithionite, and the resulting spectrum (λ_{max} 414 nm) is identical in all cases. In the presence of CO, the spectrum obtained upon addition of dithionite is that of the ferrous−CO (P450) complex, with a λ_{max} at 445 nm. The stability of this complex depends to a large extent on the presence of H_4B. H_4B-bound $iNOS_{heme}$, in the presence or absence of arginine, forms a stable P450 complex (unchanged after more than 1 h), with only a shoulder at 420 nm (P420). Pterin-

Scheme 1: Tetrahydropterin Structures

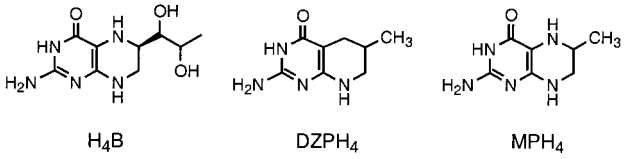

free $iNOS_{heme}$, on the other hand, forms a ferrous−CO complex with a significant P420 component that increases over time. The exact nature of the P420 complex is not known, but it is thought to arise from distortion or breaking of the thiolate−heme iron bond. This effect of pterin on the stability of the P450 complex has previously been described (*58*, *59*).

Substrate Binding Affinity. As described above, addition of substrate to H_4B-bound $iNOS_{heme}$ results in a low- to high-spin state conversion of the heme, as evidenced by a decrease in absorbance at ~420 nm and an increase in absorbance at ~382 nm in the difference spectrum. These spectral changes are dependent on the concentration of substrate added and were used to determine the affinity of H_4B-bound $iNOS_{heme}$ for both substrates. Fitting of the titration data yields K_d values of 5.8 ± 1.6 μM for arginine ($n = 10$) and 1.5 ± 0.3 μM for NHA ($n = 9$). The affinity of $iNOS_{heme}$ for substrate is similar to that reported for full-length iNOS, where the K_d values were determined to be 14 μM for arginine and 3 μM for NHA (*33*). Both substrates also bind to pterin-free $iNOS_{heme}$, but with much poorer affinity. A small spectral change is observed on addition of 1 mM arginine, but the resulting spectrum is still that of mostly low-spin heme. Similar results are obtained with NHA, and a K_d of 700 μM was determined for the binding of this substrate to pterin-free $iNOS_{heme}$. An effect of pterin on the binding affinity for substrate is expected and consistent with previous observations with full-length NOS that show cooperativity in pterin and substrate binding and in their ability to effect a spin-state change of the NOS heme (*32*−*34*, *60*, *56*).

Binding Affinity for $DZPH_4$ and MPH_4. Pterin-free $iNOS_{heme}$ was titrated with the redox-stable pterin analogue, $DZPH_4$ (Scheme 1). The addition of $DZPH_4$ effects a low- to high-spin shift of the heme, evidenced by a decrease in absorbance at 423 nm and an increase at 388 nm in the difference spectrum. In contrast to the binding of H_4B (*61*, *62*), binding of $DZPH_4$ to $iNOS_{heme}$ is complete in the time required for mixing and does not require the presence of a thiol, as observed for full-length iNOS (*62*). Fitting of the titration data yields a K_d of 80.1 ± 19.0 μM ($n = 6$). The presence of 1 mM arginine lowers the K_d about 2-fold, to 39.1 ± 0.4 μM ($n = 3$). Arginine has previously been shown to increase the affinity of full-length NOS for both H_4B (3- to 7-fold; *32*, *56*) and $DZPH_4$ (~2-fold, *62*). The lower affinity of NOS for $DZPH_4$ is likely due to the substitution of a methyl group at the 6-position of the pteridine ring for the dihydroxypropyl side-chain of H_4B (*58*, *62*).

The binding of MPH_4 to pterin-free $iNOS_{heme}$ was also examined. The binding of this pterin is slow and requires the presence of a thiol. A K_d for the binding of MPH_4 to pterin-free $iNOS_{heme}$ was not determined here, but a similar decrease in affinity is expected for this 6-methyl substituted pterin as observed for $DZPH_4$.

Native Molecular Weight of $iNOS_{heme}$. The oligomeric state of $iNOS_{heme}$ was examined by analytical gel filtration. The standards had retention times of 5.75 min (thyroglobulin), 6.30 min (apoferritin), 7.21 min (alcohol dehydrogenase), 7.45 min (bovine serum albumin), 7.82 min (egg albumin), and 8.36 min (carbonic anhydrase). Dimeric and monomeric forms of $iNOS_{heme}$ can be separated by this method, with dimer (apparent molecular mass of 113 kDa) eluting at 7.25 min and monomer (apparent molecular mass of 57 kDa) eluting at 7.75 min. Both H_4B-bound and pterin-free $iNOS_{heme}$, as well as the imidazole-bound (as purified) $iNOS_{heme}$, are primarily dimeric (data not shown). These results indicate that the interactions between NOS subunits that lead to dimerization are preserved in the isolated heme domain. The addition of 25% glycerol to any of these forms causes $iNOS_{heme}$ to elute at 6.52 min, corresponding to an apparent molecular mass of 290 kDa. This may represent tetrameric $iNOS_{heme}$, but it is not clear whether this oligomeric form is relevant to NOS catalysis. Results on native gels parallel those observed with gel filtration (not shown).

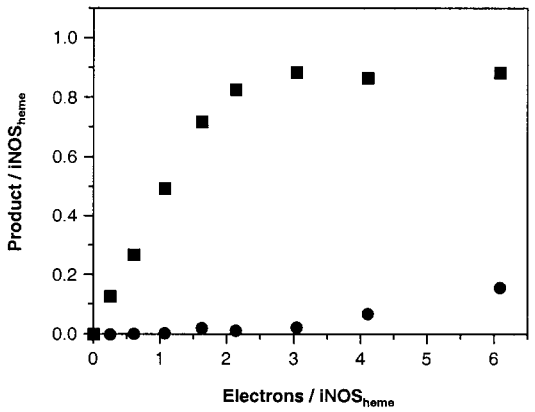

FIGURE 1: Dithionite-dependent reaction of H_4B-bound $iNOS_{heme}$ with arginine. After mixing the samples with oxygenated buffer to initiate the reaction, assays contained 40 μM H_4B-bound $iNOS_{heme}$, 1 mM arginine, and 0−120 μM dithionite. H_4B-bound $iNOS_{heme}$ catalyzes the formation of NHA (■); this reaction is linearly dependent on the concentration of added dithionite. At high dithionite concentrations, citrulline (●) is also observed. The maximum amount of products formed in this representative experiment was 0.88 equiv of NHA and 0.16 equiv of citrulline.

Dithionite-Dependent Enzyme Reactions. The ability of $iNOS_{heme}$ to catalyze product formation from either arginine or NHA was examined, using sodium dithionite as the reductant.

(A) Arginine Reactions. Reactions of H_4B-bound $iNOS_{heme}$ containing 1 mM arginine were analyzed for product formation (Figure 1). As expected, the primary product of this reaction is NHA. The amount of NHA formed increases linearly with the dithionite concentration and reaches a maximum of 0.93 ± 0.12 equiv (NHA per $iNOS_{heme}$ monomer, $n = 6$) under these conditions. Maximal NHA formation requires between 2 and 2.5 electrons per $iNOS_{heme}$. Citrulline is also formed in this reaction but only appears at high dithionite concentrations. The maximum amount of citrulline formed is 0.18 ± 0.04 equiv ($n = 4$) with the addition of 6 electrons per $iNOS_{heme}$. Identical reactions with pterin-free $iNOS_{heme}$ were also analyzed for product formation. No amino acid products were observed in these reactions, even at the highest dithionite concentration used (4 electrons per $iNOS_{heme}$; data not shown).

The ability of other pterins (Scheme 1) to support this reaction was examined, using pterin-free $iNOS_{heme}$ recon-

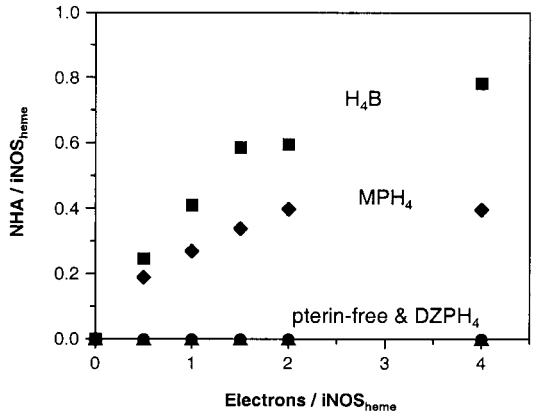

FIGURE 2: Ability of tetrahydropterins to reconstitute the activity of pterin-free iNOS$_{heme}$. Reactions contained 33 μM iNOS$_{heme}$, 1 mM arginine, and 0−66 μM dithionite. Pterin-free iNOS$_{heme}$ was reconstituted under anaerobic conditions with the indicated tetrahydropterins. In the presence of 100 μM H_4B (■) or 250 μM MPH_4 (♦), pterin-free iNOS$_{heme}$ catalyzes the formation of NHA. No products were observed in reactions of pterin-free iNOS$_{heme}$ (●) or those containing 250 μM $DZPH_4$ (▲). Concentrations given are those after mixing with oxygenated buffer.

stituted with pterin in the absence of thiol and oxygen. $DZPH_4$ lacks the N5 nitrogen and is stable to molecular oxygen. It has previously been used to study the reaction of phenylalanine hydroxylase, and has been shown to be unable to participate in the hydroxylation of the aromatic amino acid substrate (*46*). In studies with NOS, $DZPH_4$ inhibited the NADPH-dependent oxidation of arginine catalyzed by pterin-deficient iNOS (binding a substoichiometric amount of H_4B). This inhibition was competitive with H_4B (*14*). More recent studies using the recombinant pterin-free iNOS from *E. coli* have shown that $DZPH_4$ does not support citrulline formation from arginine (*63*). $DZPH_4$ has a methyl group at the 6-position, in place of the dihydroxypropyl side-chain found in H_4B. The identity of the side-chain has a significant effect on the affinity of pterin binding to NOS (*58*, *62*). For this reason, parallel reactions were carried out with the redox-active MPH_4, which also has the 6-methyl substitution and is expected to bind to NOS with similar affinity to that determined for $DZPH_4$.

The concentration of $DZPH_4$ and MPH_4 in the incubations was 500 μM, chosen on the basis of the K_d for $DZPH_4$ determined above (~40 μM in the presence of arginine). Identical reactions contained pterin-free iNOS$_{heme}$ or iNOS$_{heme}$ reconstituted with H_4B, $DZPH_4$, or MPH_4. The results from this experiment are shown in Figure 2. Under the conditions of the experiment, NHA is the sole product of these reactions, and its formation is dependent on the concentration of dithionite added. Only the redox-active pterins, H_4B and MPH_4, support the hydroxylation of arginine. No reaction was observed with pterin-free iNOS$_{heme}$ or with iNOS$_{heme}$ in the presence of $DZPH_4$. The maximum amount of NHA formed is greater with H_4B (0.75 equiv) than with MPH_4 (0.39 equiv). This difference in activity might indicate that only a small amount of MPH_4 is bound to iNOS$_{heme}$ under these conditions; alternatively, MPH_4 might be less effective than H_4B at supporting the hydroxylation of arginine.

To distinguish between these possibilities, the amount of pterin in the reconstitution was varied from substoichiometric to saturating concentrations (340 μM for H_4B, 1 mM for $DZPH_4$ and MPH_4). Spectra recorded after the incubation

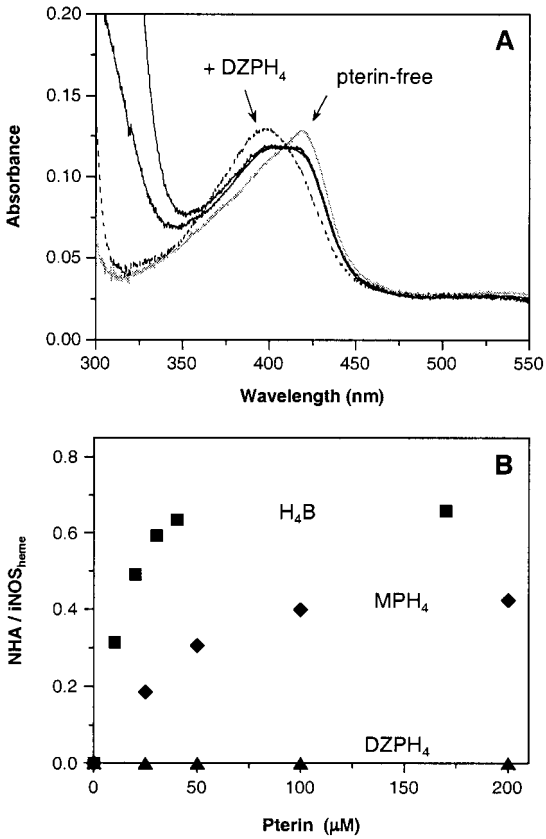

FIGURE 3: (A) Effect of tetrahydropterins on the spectrum of pterin-free iNOS$_{heme}$. Pterin-free iNOS$_{heme}$ (15 μM) was incubated under anaerobic conditions with pterin and 1 mM arginine. Spectra were recorded after 2 h incubation time; a 0.1-cm path length cuvette was used to avoid dilution of the samples, which might result in dissociation of the bound pterin. Pterin-free iNOS$_{heme}$ incubated with buffer alone (shaded spectrum) has a λ_{max} at 420 nm, indicative of mostly low-spin heme. Addition of $DZPH_4$ (1 mM) results in the greatest spectral change, with a full shift of the heme to high-spin (dashed spectrum, λ_{max} at 397 nm). Samples containing 1 mM MPH_4 or 340 μM H_4B have nearly identical spectra (solid spectra), with a broad Soret peak between 400 and 420 nm. This spectrum corresponds to ~60% high-spin heme. (B) Dependence of the arginine reaction on pterin concentration. Pterin-free iNOS$_{heme}$ was incubated under anaerobic conditions for 2 h with various concentrations of pterin. Reactions contained 40 μM iNOS$_{heme}$, 1 mM arginine, 40 μM dithionite, and 0−500 μM of the indicated pterin. $DZPH_4$ (▲) is unable to support the hydroxylation of arginine, even at concentrations where a full spectral shift is observed. NHA is formed in the presence of either H_4B (■, 0.65 equiv) or MPH_4 (♦, 0.39 equiv); the reaction is dependent on the pterin concentration.

confirm that all of the pterins bind to iNOS$_{heme}$ under these conditions (Figure 3A). Addition of 1 mM $DZPH_4$ to pterin-free iNOS$_{heme}$ results in full conversion of the heme to the high-spin state, even in the absence of thiol (λ_{max} at 397 nm). The spectra of iNOS$_{heme}$ incubated with 340 μM H_4B or 1 mM MPH_4 are nearly superimposable (except for the spectral contributions of the free pterin) and have a broad Soret peak in the range of 400−420 nm. The observed spectral changes are ~60% of the spectral shift observed when iNOS$_{heme}$ is reconstituted aerobically in the presence of DTT (data not shown), consistent with reports that a thiol is required for complete pterin reconstitution of NOS (*61*, *62*). Addition of dithionite to each of these iNOS$_{heme}$ preparations results in full heme reduction (λ_{max} at 414 nm, not shown).

Figure 3B shows the dependence of product formation on pterin concentration. The indicated pterin concentrations are

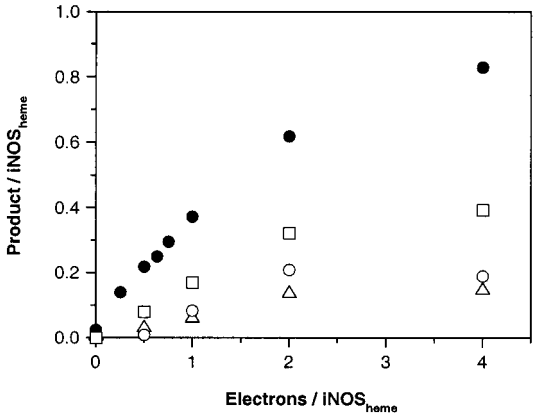

FIGURE 4: Dithionite-dependent reaction of $iNOS_{heme}$ with NHA. Reaction mixtures contained 40 μM $iNOS_{heme}$, 1 mM NHA, and 0−80 μM dithionite. Both H_4B-bound and pterin-free iNOS heme domain catalyze NHA oxidation under these conditions, and product formation in both cases is dependent on the concentration of added dithionite. With H_4B-bound $iNOS_{heme}$ (solid symbols), the sole amino acid product is citrulline (●). Pterin-free $iNOS_{heme}$ (open symbols) catalyzes the formation of a mixture of products: CN-orn (□), citrulline (○), and an unidentified amino acid (△). The maximum amount of amino acid product formed in this representative experiment was 0.83 equiv for the H_4B-bound reaction and 0.77 equiv for the pterin-free reaction.

those after mixing with oxygenated buffer, with all reactions containing 40 μM $iNOS_{heme}$ and 40 μM dithionite (2 electrons per $iNOS_{heme}$). As reported above, no product was formed in reactions containing $DZPH_4$. In the presence of H_4B or MPH_4, NHA formation increases with the pterin concentration before reaching saturation. Saturation with H_4B is reached at 40 μM of added pterin, and the maximum product formed is 0.65 equiv (NHA per $iNOS_{heme}$). Saturation with MPH_4 requires 200 μM pterin, and the maximum product formed is 0.42 equiv. Taken together with the spectral data, which show that H_4B and MPH_4 bind to the same extent in this experiment, these results indicate that the difference in activity between the two pterins is not due to differences in their binding to $iNOS_{heme}$.

(B) NHA Reactions. Similar dithionite-dependent reactions were carried out in the presence of 1 mM NHA. As with the arginine reactions, product formation in this case also requires dithionite (Figure 4). The sole amino acid product of NHA oxidation for H_4B-bound $iNOS_{heme}$ is citrulline. The amount of citrulline formed increases linearly with the dithionite concentration and reaches a maximum between 2 and 2.5 electrons added per $iNOS_{heme}$. The maximum amount of citrulline formed under these conditions is 0.83 ± 0.08 equiv (citrulline per $iNOS_{heme}$, $n = 8$). The oxidation of NHA catalyzed by pterin-free $iNOS_{heme}$ leads to different products than those observed with H_4B-bound $iNOS_{heme}$. Citrulline is formed, but it is no longer the sole amino acid product. The predominant product of the reaction is CN-orn, and a third amino acid is also formed. This amino acid (retention time of 6.9 min) has previously been observed in the peroxide-dependent oxidation of NHA catalyzed by $iNOS_{heme}$ (A. R. Hurshman and M. A. Marletta, unpublished results). Its identity has not been conclusively determined, but coupled HPLC/MS analysis of the reaction products suggests that it may represent a dihydroxylated arginine species (A. R. Hurshman and M. A. Marletta, unpublished results). Although the identity of the amino acid products differs in the

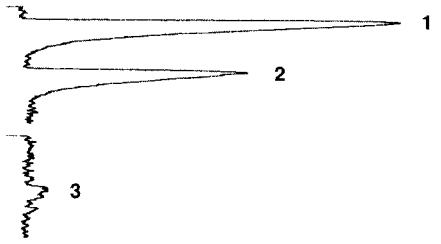

FIGURE 5: •NO formation from dithionite-dependent NHA oxidation. Reactions containing 40 μM $iNOS_{heme}$, 1 mM NHA, and 40 μM dithionite were analyzed for the presence of •NO. Injections (50−100 μL) were made from the headspace of the reaction vials immediately after oxygenation. The upper chromatogram shows the formation of •NO in the reaction catalyzed by H_4B-bound $iNOS_{heme}$; peak 1 corresponds to a 100 μL injection, and peak 2 is a 50 μL injection from the same reaction. In contrast, •NO is not formed in the reaction of pterin-free $iNOS_{heme}$ with NHA (100 μL, peak 3). The small peak observed represents at most 5% of the signal observed with H_4B-bound $iNOS_{heme}$.

pterin-free reaction, the amount of product formed (sum of the three amino acids) is similar. Maximum product formation in the pterin-free reaction is 0.75 ± 0.01 equiv (amino acid product per $iNOS_{heme}$, $n = 4$) and requires between 2 and 2.5 electrons added per $iNOS_{heme}$.

Reaction mixtures were also analyzed for the inorganic product of NHA oxidation. •NO was detected by chemiluminescence, which is very sensitive and specific for •NO. The headspace of the reaction vials was analyzed for •NO formation because •NO formed in these reactions rapidly partitions to the gas phase, and injections from the aqueous phase gave a much lower signal. Maximal •NO concentration was detected when the headspace was sampled within 1 min of mixing with oxygenated buffer. Analysis of the reactions of H_4B-bound and pterin-free $iNOS_{heme}$ is shown in Figure 5. Although •NO is easily detected in the reactions of H_4B-bound $iNOS_{heme}$, the signal observed for identical reactions with pterin-free $iNOS_{heme}$ is small. At most, this signal represents 5% of that observed for H_4B-bound $iNOS_{heme}$. The inorganic product of the pterin-free reaction is probably NO^- rather than •NO, as previously reported for the NADPH-dependent oxidation of NHA by pterin-free iNOS (*35*).

The inorganic product was quantified as NO_2^-/NO_3^-, the stable decomposition products of •NO. Previous results from our laboratory have shown that NO^- formed either in the peroxide-dependent reaction of H_4B-bound iNOS (*17*, *18*) or in the NADPH-dependent reaction of pterin-free iNOS (*35*) can also be converted to NO_2^-/NO_3^-. The products of the dithionite-dependent reactions of $iNOS_{heme}$ with NHA are shown in Figure 6. The maximum amount of NO_2^-/NO_3^- formed in the H_4B-bound $iNOS_{heme}$ reaction is 0.56 ± 0.11 equiv (NO_2^-/NO_3^- per $iNOS_{heme}$, $n = 6$), and the stoichiometry of amino acid to inorganic product varies from 1.5:1 to 2:1 (Figure 6A). This observed stoichiometry is higher than the expected 1:1 for the formation of citrulline and •NO and can be explained by escape or incomplete conversion of gaseous •NO to its aqueous decomposition products. The maximum amount of NO_2^-/NO_3^- detected in the reactions of pterin-free $iNOS_{heme}$ is 0.38 ± 0.06 equiv ($n = 2$), and the stoichiometry of amino acid to inorganic product in this reaction ranges from 2:1 to 2.5:1 (Figure 6B). NO^- is not volatile, but it can decompose by dimerization and dehydration to form N_2O (*64*, *65*). Analysis of NO_2^-/NO_3^- alone is likely to underestimate the total amount of NO^- formed;

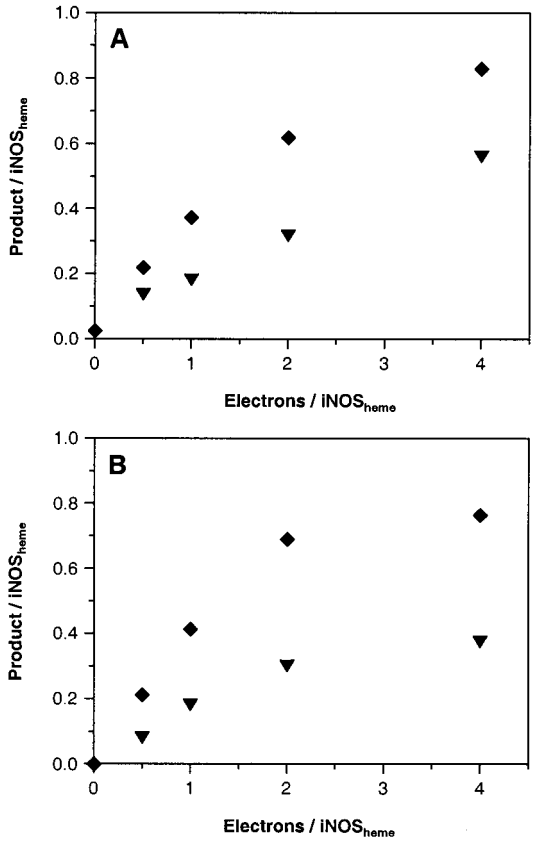

FIGURE 6: Stoichiometry of amino acid and inorganic product in the dithionite reaction of $iNOS_{heme}$ with NHA. Reactions contained 40 μM $iNOS_{heme}$, 1 mM NHA, and 0−80 μM dithionite. The sum of amino acid products (♦) and NO_2^-/NO_3^- (▼) are shown as a function of electron equiv. (A) The stoichiometry of amino acid to inorganic product varies from 1.5:1 to 2:1 in reactions of H_4B-bound $iNOS_{heme}$. The maximum amount of NO_2^-/NO_3^- formed is 0.56 equiv. (B) With pterin-free $iNOS_{heme}$, the inorganic product of the reaction is also detected as NO_2^-/NO_3^-, even though •NO is not formed. The stoichiometry of amino acid to inorganic product varies from 2:1 to 2.5:1, with a maximum of 0.38 equiv NO_2^-/NO_3^-.

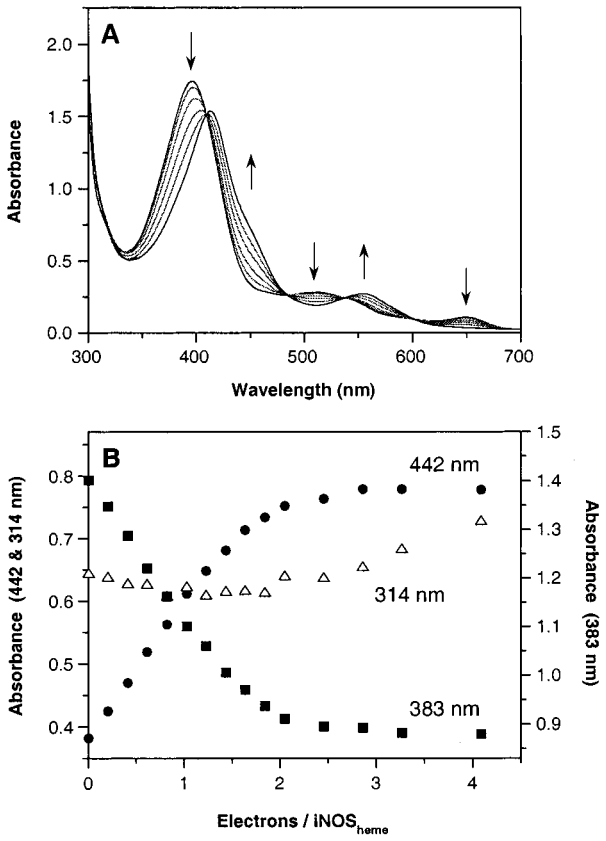

FIGURE 7: Dithionite titration of H_4B-bound $iNOS_{heme}$ in the presence of arginine. This representative titration contained 20.5 μM H_4B-bound $iNOS_{heme}$, 1 mM arginine, 250 μM PCA, and 1.2 U PCD in 1.5 mL total volume. (A) Upon addition of sodium dithionite to the sample, the spectrum of $iNOS_{heme}$ shifts from the high-spin ferric form (λ_{max} at 396 nm) to the ferrous species (λ_{max} at 414 nm). Several intermediate spectra are shown, and the arrows indicate the direction of the spectral changes with increasing dithionite. The calculated difference spectra show a decrease at 383 nm and concomitant increase at 442 nm upon reduction (not shown). Smaller changes are also observed at 511, 566, and 650 nm. (B) The absorbance changes at 383 and 442 nm are plotted as a function of electron equiv added. The number of electrons required to fully reduce the heme of $iNOS_{heme}$ was determined from the intersection of two lines drawn through the data points, one line representing the slope of the reduction curve and the second line drawn through the absorbance value reached upon full reduction. Full reduction in this experiment required 2.0 electrons; the addition of more dithionite results in an increase in absorbance at 314 nm (excess dithionite present) with no further changes in the heme Soret.

reactions were not analyzed for N_2O. Another factor to consider in the pterin-free reaction is that ~25% of the amino acid formed is an unidentified product. If this product is a dihydroxylated amino acid, the expected stoichiometry of products would be ~1.3:1 (assuming 1:1 stoichiometry for the citrulline and CN-orn formed, and no inorganic product for the unknown).

Dithionite Titrations. $iNOS_{heme}$ was titrated with sodium dithionite to determine the number of electron equivalents required to fully reduce $iNOS_{heme}$ under various conditions.

(A) H_4B-bound $iNOS_{heme}$. Titrations of H_4B-bound $iNOS_{heme}$ were carried out both in the absence of substrate and in the presence of 1 mM either arginine or NHA. Figure 7 is a representative titration of H_4B-bound $iNOS_{heme}$ in the presence of arginine. Similar results were also obtained with NHA and in the absence of substrate (not shown). Upon addition of sodium dithionite, the spectrum of $iNOS_{heme}$ shifts from the high-spin ferric form (λ_{max} at 396 nm) to the ferrous species (λ_{max} at 414 nm). Several intermediate spectra are shown (Figure 7A), and the arrows indicate the direction of the spectral changes with increasing dithionite. The difference spectra show a decrease at 383 nm and concomitant increase at 442 nm upon reduction, and the absorbance changes at these two wavelengths are plotted as a function of electron equiv added (Figure 7B). Full reduction requires 2 to 2.5 electrons per $iNOS_{heme}$; the addition of more dithionite results in an increase in absorbance at 314 nm (excess dithionite present) with no further changes in the heme Soret. Since the heme cofactor can only be reduced by one electron, any additional electrons must be reducing another site on the enzyme, perhaps the pterin cofactor or a protein disulfide. The spectral changes observed are linear over almost the entire course of the titration, indicating that both $iNOS_{heme}$ redox sites are being reduced simultaneously by dithionite or that there is rapid equilibration between the two sites. The number of electrons required for full reduction of H_4B-bound $iNOS_{heme}$ varies from 2 to 2.5, suggesting a variable amount of oxidation of protein thiols or the pterin cofactor in different enzyme preparations.

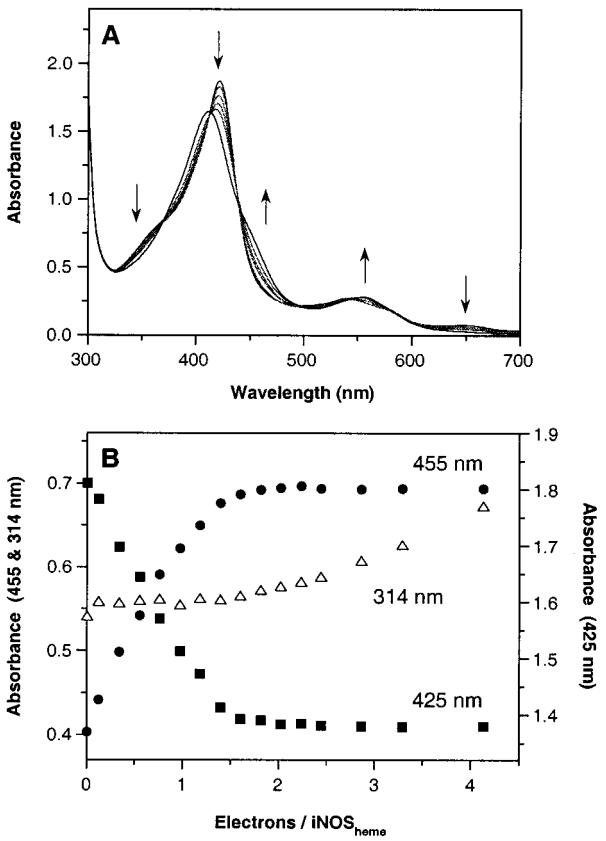

FIGURE 8: Dithionite titration of pterin-free $iNOS_{heme}$ in the absence of substrate. This representative titration contained 23.1 μM H_4B-bound $iNOS_{heme}$, 250 μM PCA, and 1.2 U PCD in 1.5 mL total volume. (A) Upon addition of dithionite, the spectrum shifts from the predominantly low-spin ferric species (λ_{max} at 421 nm) to the same ferrous form observed with H_4B-bound $iNOS_{heme}$ (λ_{max} at 414 nm). Several intermediate spectra are shown, and the arrows indicate the direction of the spectral changes with increasing dithionite. The calculated difference spectra show a decrease at 425 nm and concomitant increase at 445 nm upon reduction (not shown). Smaller changes are also observed at 355, 560, and 650 nm. (B) The absorbance changes at 425 and 445 nm are plotted as a function of electron equiv added. The number of electrons required to fully reduce the heme of $iNOS_{heme}$ was determined from the intersection of the line representing the initial slope of the reduction curve and the line drawn through the absorbance value reached upon full reduction. Full reduction in this experiment required 1.3 electrons; the addition of more dithionite results in an increase in absorbance at 314 nm (excess dithionite present) with no further changes in the heme Soret.

(B) Pterin-Free $iNOS_{heme}$. Figure 8 shows a titration of pterin-free $iNOS_{heme}$ in the absence of substrate. The initial spectrum has an absorbance maximum at 421 nm (Figure 8A). Upon addition of dithionite, the spectrum shifts from this predominantly low-spin ferric species to the same ferrous form observed with H_4B-bound $iNOS_{heme}$ (λ_{max} at 414 nm). Maximal changes in the difference spectra occur at 425 and 455 nm; the absorbance changes at these two wavelengths are plotted in Figure 8B as a function of electron equiv added. In contrast to the reduction of H_4B-bound $iNOS_{heme}$, full heme reduction for pterin-free $iNOS_{heme}$ requires only 1 to 1.5 electrons per $iNOS_{heme}$. Excess dithionite (λ_{max} at 314 nm) is apparent in the spectra at higher dithionite concentrations, and no further changes in the heme Soret are observed. Similar results were obtained with pterin-free $iNOS_{heme}$ in the presence of 1 mM arginine or NHA (data not shown). Titrations in the presence of substrate were complicated by the heterogeneity of these samples, since the addition of substrate to pterin-free $iNOS_{heme}$ results in only a partial shift to high-spin, and the spectral changes upon reduction differ depending on the spin state of the heme.

Dependence of Product Formation on Reduction of $iNOS_{heme}$. Product formation in the reactions described above (Figures 1, 2, and 4) and reduction of $iNOS_{heme}$ (Figures 7 and 8) both show a linear dependence on the concentration of added dithionite. The data from these experiments were replotted, to directly compare product formation with $iNOS_{heme}$ reduction. The amount of product formed at each concentration of dithionite was plotted vs the extent of reduction of $iNOS_{heme}$ determined from the titration curves at the corresponding dithionite concentration.

(A) Arginine Reactions. The amount of NHA formed in reactions of H_4B-bound and pterin-free $iNOS_{heme}$ as a function of $iNOS_{heme}$ reduction is shown in Figure 9A. For H_4B-bound $iNOS_{heme}$, there is a clear correlation between product formation and the extent of $iNOS_{heme}$ reduction. The data points shown correspond to dithionite concentrations up to 2 electrons per $iNOS_{heme}$, where reduction and product formation are substoichiometric relative to $iNOS_{heme}$. Linear regression of these data points gives a slope of 0.89 ± 0.01, suggesting that the theoretical product stoichiometry is 1 equiv of NHA per reduced $iNOS_{heme}$. At higher dithionite concentrations, where $iNOS_{heme}$ is fully reduced but excess reducing equivalents are present, a linear relationship is no longer observed (product formation continues to increase slightly, but the extent of reduction cannot be higher than 1.0). A similar plot of the pterin-free $iNOS_{heme}$ data is also shown in Figure 9A. The slope of this line is 0, since no NHA is observed in the pterin-free $iNOS_{heme}$ reactions, even when $iNOS_{heme}$ is fully reduced.

(B) NHA Reactions. Data were similarly plotted for the reactions with NHA as the substrate. Figure 9B shows the dependence of product formation on $iNOS_{heme}$ reduction in both H_4B-bound and pterin-free $iNOS_{heme}$. Product formation for H_4B-bound $iNOS_{heme}$ refers to citrulline only, whereas that for pterin-free $iNOS_{heme}$ represents the sum of the three amino acid products. The data points shown are only those where no excess dithionite was present. Linear regression of the data gives a slope of 0.83 ± 0.03 for H_4B-bound $iNOS_{heme}$ and a slope of 0.53 ± 0.02 for pterin-free $iNOS_{heme}$. The slope of the H_4B-bound data is similar to that obtained for the arginine reaction, suggesting that the theoretical stoichiometry of product formation in the NHA reaction is probably 1 equiv of citrulline per reduced $iNOS_{heme}$. The significantly lower slope determined for the pterin-free reactions indicates that the expected product stoichiometry in this reaction is only 0.5 amino acid product per reduced $iNOS_{heme}$.

DISCUSSION

We have used $iNOS_{heme}$ to examine the mechanism of both steps of the NOS reaction. The heme domain of iNOS was expressed in *E. coli* and purified by a three-column procedure. Characterization of the heterologously expressed $iNOS_{heme}$ shows it to behave in all respects like full-length iNOS. In particular, the heme environment is indistinguishable from that of iNOS, the substrate- and pterin-binding sites appear intact, and the domain is able to form a stable

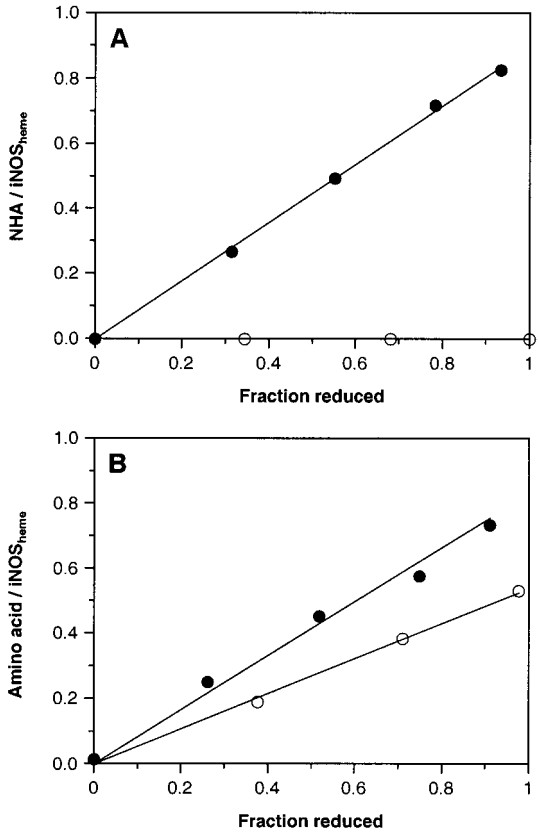

FIGURE 9: Dependence of product formation on $iNOS_{heme}$ reduction. Dithionite assays and titrations were carried out as described in the Experimental Procedures. Product formation at a given dithionite concentration (from dithionite assays) was plotted vs the extent of reduction calculated from spectra obtained at the corresponding dithionite concentration (from titrations). (A) Arginine reactions. NHA formation in reactions containing 1 mM arginine is shown for either H_4B-bound (●) or pterin-free (○) $iNOS_{heme}$ at various fixed concentrations of dithionite (corresponding to 0, 0.6, 1.1, 1.5, and 2.1 electron equiv for H_4B-bound reactions and 0, 0.5, 1.0, and 1.5 electron equiv for pterin-free reactions). NHA formation in reactions of H_4B-bound $iNOS_{heme}$ shows a linear dependence on $iNOS_{heme}$ reduction; the slope of the line is 0.89 ± 0.01. The identical plot for pterin-free $iNOS_{heme}$ has a slope of 0, because no NHA is formed in these reactions, even when $iNOS_{heme}$ is fully reduced. (B) NHA reactions. Reactions of H_4B-bound (●) or pterin-free (○) $iNOS_{heme}$ contained 1 mM NHA and various fixed concentrations of dithionite (corresponding to 0, 0.5, 1.0, 1.5, and 2.0 electron equiv for H_4B-bound reactions and 0, 0.5, 1.0, and 1.5 electron equiv for pterin-free reactions). Product formation in both of these reactions shows a linear dependence on $iNOS_{heme}$ reduction. The product of NHA oxidation by H_4B-bound $iNOS_{heme}$ is citrulline; linear regression of the data points gives a slope of 0.83 ± 0.03. Product in the pterin-free reactions is plotted as the sum of the three amino acid products; the slope of the line through these data is 0.53 ± 0.02.

dimer. Because *E. coli* have no endogenous H_4B, $iNOS_{heme}$ is isolated without any bound pterin but can be readily reconstituted with H_4B or other pterins. Both pterin-bound and pterin-free forms of $iNOS_{heme}$ were used in these studies to investigate the role of H_4B in the enzyme reaction.

We examined the ability of $iNOS_{heme}$ to catalyze the hydroxylation of arginine and the oxidation of NHA. In the absence of the reductase domain and its bound flavin cofactors, $iNOS_{heme}$ cannot accept electrons from NADPH, so reactions were carried out with sodium dithionite as the reductant. The rapid reaction of dithionite with oxygen precludes studying the dithionite-dependent reactions of $iNOS_{heme}$ under normal assay conditions, since both the oxygen and the dithionite necessary for catalysis would be depleted. Instead, the dithionite-dependent reactions of $iNOS_{heme}$ are effectively single turnover experiments, where $iNOS_{heme}$ is reduced anaerobically and subsequently oxygenated to initiate the reactions. H_4B-bound $iNOS_{heme}$ catalyzes both steps of the NOS reaction under these conditions, hydroxylating arginine to NHA, and converting NHA to citrulline and •NO. Both reactions are dependent on the addition of dithionite, requiring between 2 and 2.5 electron equivalents to form 1 equivalent of product.

Hydroxylation of arginine by $iNOS_{heme}$ shows an absolute dependence on the presence of a bound, reduced pterin. This requirement for pterin is consistent with previous reports that pterin-free iNOS does not catalyze an NADPH-dependent reaction with arginine (*35*). Furthermore, it appears that the function of H_4B in this step of the NOS reaction is dependent on the redox properties of the pterin. Only the redox-active pterins used in this study (H_4B and MPH_4) are able to support catalysis. $DZPH_4$, which is stable to molecular oxygen, does not support the reaction with arginine. Several alternative explanations for these data can be ruled out. Although the affinity of binding of both biopterin analogues is significantly lower than that of H_4B for NOS, the spectral studies indicate that all of the pterins used are able to bind to $iNOS_{heme}$ under the experimental conditions. In fact, the extent of binding of the pterins following anaerobic reconstitution does not correlate with their ability to support the hydroxylation of arginine. $DZPH_4$ binding to $iNOS_{heme}$ is fast and effects a complete shift of the heme to the high-spin state, but the $DZPH_4$-bound $iNOS_{heme}$ does not form any NHA. In contrast to that result, H_4B and MPH_4 cause a smaller spectral change upon binding to $iNOS_{heme}$, suggesting that the pterin-binding site is not fully occupied in these samples. However, both H_4B- and MPH_4-bound $iNOS_{heme}$ can hydroxylate arginine. A second concern is the effect of each pterin on the redox potential of the heme cofactor. H_4B is reported to cause an increase of 52 mV in the midpoint potential of the heme of $iNOS_{heme}$ (*36*), and other pterins may have a similar effect. Modulation of the heme potential by the various pterins was not directly examined in these experiments, but full reduction of all of the $iNOS_{heme}$ samples was observed in the presence of dithionite (2 electrons per $iNOS_{heme}$). It is thus unlikely that effects of the pterin on heme reduction are responsible for the observed differences in activity.

A comparison of the binding and activity of the three pterins examined here gives some clues regarding the essential features of the pterin structure required for NOS catalysis. The substituent at the 6-position is important for high-affinity binding of the pterin cofactor to NOS. Replacement of the native dihydroxypropyl side-chain present in H_4B with a methyl group (MPH_4 and $DZPH_4$) causes a significant decrease in binding affinity, consistent with earlier reports (*58*, *62*). Additionally, MPH_4 has lower activity ($\sim$ 65%) than H_4B in the arginine reactions, even when each pterin is present at saturating concentrations. This result suggests that the dihydroxypropyl side-chain is required for efficient function of the pterin cofactor, perhaps by optimally orienting the pterin in the active site. However, the key determinant of pterin activity in these reactions is the presence of a nitrogen atom at the 5-position of the pterin ring. This nitrogen is essential for the redox properties of the pterin

cofactor, and replacement of N5 with a methylene group (as in $DZPH_4$) results in a pterin that is stable to molecular oxygen. This substitution also completely abolishes activity of the pterin in the arginine reaction of $iNOS_{heme}$, suggesting that this reaction requires a redox-active pterin. There is no structural information available to date concerning the binding of either MPH_4 or $DZPH_4$ to NOS, so it is not clear how these substitutions may affect the hydrogen bonding interactions and the overall structure of the NOS active site. Although the redox properties of the pterin appear to be essential for NOS catalysis, conclusive interpretation concerning the importance and the function of N5 of the pterin requires additional structural data.

The stoichiometry of product formation relative to dithionite-derived electrons (0.93 equiv of NHA formed in the presence of 2 to 2.5 electron equiv) in the arginine reaction of H_4B-bound $iNOS_{heme}$ is lower than expected. The hydroxylation of arginine requires two electrons, but if the pterin cofactor provides any reducing equivalents in this reaction, as suggested by the requirement for a redox-active tetrahydropterin, the number of dithionite-derived electrons required for one turnover should be less than 2. Reductive titrations of H_4B-bound $iNOS_{heme}$ with dithionite indicate that 2 to 2.5 electrons are apparently required to fully reduce the heme. The heme cofactor itself can only be reduced by one electron, so any additional electrons must be reducing another site on the enzyme. Full reduction of pterin-free $iNOS_{heme}$ only requires 1 to 1.5 electrons; therefore, it seems likely that some pterin oxidation occurs during preparation of H_4B-bound $iNOS_{heme}$ samples. However, pterin oxidation alone cannot explain the titration results, since reduction of pterin-free samples also requires more than 1 electron. The most likely explanation for these observations is provided by crystallographic data of the NOS heme domain in the absence of any bound zinc (*26*, *23*). These structures show an intersubunit disulfide bond between two of the cysteine ligands from the zinc tetrathiolate site. Our $iNOS_{heme}$ samples are zinc deficient (0.46 per dimer). If cysteine oxidation occurs in the absence of bound zinc to form an intersubunit disulfide bond, this could account for up to 0.5 electron equiv per $iNOS_{heme}$ monomer (up to 0.5 disulfide per dimer, or 0.5 electron per monomer). There is no difference in catalytic activity between zinc-bound and zinc-free NOS preparations (*53*, *54*). However, variable oxidation of the bound pterin cofactor and of protein thiols in different enzyme preparations may account for differences in the stoichiometries (0.2−0.8 equiv of NHA formed in the presence of 1 electron equiv) previously reported for dithionite-dependent reactions (*41*, *66*). In this study, we have directly compared product formation in the dithionite-dependent reactions with the titration data to determine the product stoichiometry. The observed dependence of NHA formation on $iNOS_{heme}$ reduction (see Figure 9A) clearly demonstrates that fully reduced H_4B-bound $iNOS_{heme}$ (pterin cofactor as H_4B and heme cofactor as Fe^{II}) can catalyze the formation of 1 equiv of NHA in the absence of any additional electrons from dithionite.

These results suggest that the pterin cofactor does indeed provide reducing equivalents for the hydroxylation of arginine. One possible role for the reduced pterin is that it directly catalyzes the hydroxylation of arginine to NHA in a reaction analogous to that proposed for the aromatic amino acid hydroxylases (see refs *67*−*70*). Although this type of pterin-dependent reaction has been proposed for NOS (*27*, *28*, *14*), the ability of several N5-substituted H_4B analogues to support NOS turnover suggests that the role of H_4B in NOS is different from that in other pterin-utilizing enzymes (*71*, *72*). There is evidence that H_4B is involved in single electron transfer to the NOS heme, leading to the formation of a pterin radical (*41*, *73*, *74*). The involvement of the pterin in electron transfer in NOS was first proposed on the basis of differences in the spectral decay of the $Fe^{II}O_2$ complex of nNOS in the presence and absence of H_4B (*40*). Furthermore, a comparison of the structural features of the pterin-binding site of NOS to those of other pterin-dependent enzymes reveals unique hydrogen-bonding interactions that may stabilize a pterin radical (*21*). A pterin radical ($H_3B\bullet$) has been directly observed upon reaction of reduced $iNOS_{heme}$ with oxygen in the presence of arginine, using rapid freeze-quench EPR techniques (*41*). The radical forms under conditions where arginine hydroxylation also occurs; in fact, 0.8 NHA was formed per $iNOS_{heme}$ in reactions where the radical accumulated to 80% of the total $iNOS_{heme}$, suggesting that $H_3B\bullet$ may be an integral part of NOS catalysis. Two other reports have since appeared, confirming the formation of a pterin radical in reactions with the heme domain of nNOS (*73*) and iNOS (*74*). The latter paper further demonstrates that $H_3B\bullet$ formation precedes the appearance of NHA in these reactions.

Scheme 2: Model for the Hydroxylation of Arginine by NOS

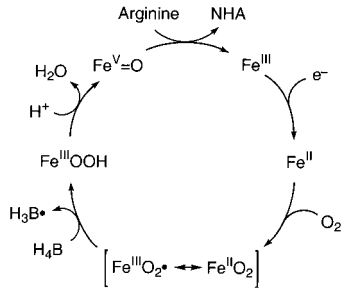

The results presented here provide additional support for the involvement of H_4B in electron transfer in the hydroxylation of arginine (Scheme 2). In this model, the first electron to reduce $iNOS_{heme}$ comes from dithionite. Following the reaction of reduced heme with oxygen, a second electron is required to form the ferric−(hydro)peroxo species. In the reactions described here with $iNOS_{heme}$, the second electron would come from the pterin, forming a pterin radical that subsequently requires reduction prior to the next turnover. Protonation of the $Fe^{III}OO(H)$ complex followed by O−O bond scission leads to the formation of the $Fe^{V}{=}O$ species, which can hydroxylate arginine. This model explains the absolute dependence of arginine hydroxylation on H_4B, particularly for full-length NOS. If H_4B is in the electron transfer pathway from the flavins to the heme, reduction of the heme may not occur efficiently in the pterin-free enzyme. This would account for the lack of reactivity of pterin-free iNOS with arginine, as well as the slow rate of NADPH-dependent heme reduction observed in pterin-free iNOS (*35*). However, the model does not fully explain why pterin-free $iNOS_{heme}$ is unable to catalyze the hydroxylation of arginine

Scheme 3: Models for the Oxidation of NHA by NOS[a]

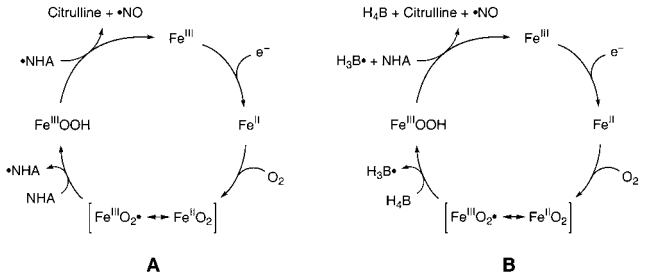

[a] Alternative models are shown for the oxidation of NHA, involving either (A) NHA or (B) H_4B as the source of the second electron for the reaction

in the presence of dithionite. It might be expected that dithionite should be able to provide both electrons to directly reduce the heme cofactor of $iNOS_{heme}$, even in the absence of H_4B. A recent paper reports the formation of citrulline and NO^- from arginine in an NADPH-dependent reaction of pterin-free nNOS (*75*). This reaction is highly uncoupled, requiring 16 mol of NADPH to form 1 mol of citrulline (or 32 electron equiv for 1 equiv of citrulline). The authors argue that the observed uncoupling results from inefficient electron transfer to the $Fe^{II}O_2$ complex in the absence of H_4B. Electron transfer from dithionite to the $Fe^{II}O_2$ complex of $iNOS_{heme}$ may also be slow or inefficient and may account for the observed lack of reactivity of pterin-free $iNOS_{heme}$ with arginine.

Dithionite reactions with NHA as the substrate demonstrate a role for pterin in this step as well. While the products of NHA oxidation by H_4B-bound $iNOS_{heme}$ are citrulline and •NO, pterin-free $iNOS_{heme}$ instead catalyzes the formation of citrulline, CN-orn, an unidentified amino acid, and NO^-. This reaction is similar to that previously characterized for pterin-free iNOS, where the products of NADPH-dependent NHA oxidation are citrulline, CN-orn, and NO^- (*35*). The stoichiometry of product formation relative to the dithionite concentration (0.83 equiv of citrulline in the presence of 2 to 2.5 electron equiv) for H_4B-bound $iNOS_{heme}$ is similar to that reported above for the arginine reactions. Reductive titrations with dithionite in the presence of NHA indicate that full reduction of the heme of $iNOS_{heme}$ also requires 2 to 2.5 electrons. Together these data clearly demonstrate that product formation is dependent on $iNOS_{heme}$ reduction (see Figure 9B) and that 1 equiv of citrulline is formed by fully reduced H_4B-bound $iNOS_{heme}$ (with H_4B and Fe^{II} heme) in the absence of any additional electrons from dithionite.

This observation is consistent with our proposal that the ferrous−dioxygen complex catalyzes the oxidation of NHA to citrulline and •NO (*2*). In this proposed mechanism, the second electron for heme reduction comes (perhaps as a hydrogen atom) from NHA, forming •NHA and $Fe^{III}OOH$ (Scheme 3A). The resulting $Fe^{III}OOH$ undergoes a nucleophilic reaction with •NHA to form a tetrahedral intermediate that decomposes to citrulline and •NO. To date, •NHA has not been detected in any reactions of NOS with NHA, so there is no direct evidence for this mechanism. Alternatively, the second electron might come from H_4B (Scheme 3B), as it does in the arginine reaction. This possibility has recently been discussed in several papers (*73*, *76*, *75*), which propose a role for H_4B in electron transfer in both steps of the NOS reaction. In rapid freeze-quench EPR experiments, H_3B• only accumulated to 2.8% of the total $iNOS_{heme}$ in the presence of NHA; under these same conditions 0.6 citrulline was formed per $iNOS_{heme}$ (*41*). Although only a small amount of H_3B• was observed in the oxidation of NHA to citrulline, we cannot exclude the possibility that H_3B• forms transiently as an intermediate in this reaction. If H_3B• does form in this reaction, it must undergo a subsequent 1-electron reduction for the reaction to yield the correct products (•NO rather than NO^-) with the observed stoichiometry. Scheme 4 shows two pathways by which this might occur. A tetrahedral intermediate is formed by nucleophilic reaction of $Fe^{III}OOH$

Scheme 4: Proposed Electron Transfer Role for H_4B in the Oxidation of NHA

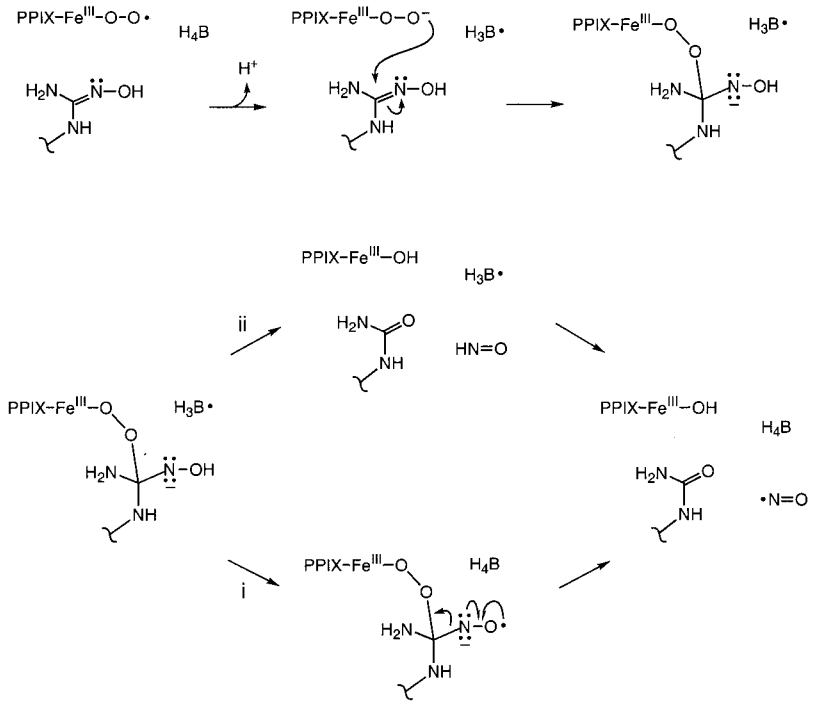

with NHA. Path (i) shows one-electron oxidation of the tetrahedral intermediate by $H_3B\bullet$, regenerating the reduced pterin (H_4B). Subsequent collapse of the oxidized intermediate releases •NO and citrulline. In path (ii), the products of the reaction are citrulline and NO^- (shown as HNO), which is then oxidized by $H_3B\bullet$ to form •NO. This second pathway requires that NO^- be efficiently trapped by $H_3B\bullet$ before it leaves the active site and seems less likely than path (i). A third pathway (not pictured in Scheme 4) involves oxidation of NO^- to •NO by the heme cofactor (*73*, *76*, *75*). The resulting $Fe^{II}NO$ complex would then be oxidized by $H_3B\bullet$ to $Fe^{III}NO$, accounting for the observation of an $Fe^{III}NO$ species in NHA reactions of nNOS (*66*, *73*, *75*) and eNOS (*76*). However, the $Fe^{III}NO$ complex is not observed in similar stopped-flow experiments with $iNOS_{heme}$ (A. R. Hurshman and M. A. Marletta, unpublished results), and it is therefore not clear whether this species is an intermediate in the NOS reaction. Any of these three pathways regenerates the reduced pterin cofactor (H_4B) and leads to the same products, citrulline and •NO. The data presented here do not distinguish among these three possibilities.

The products of the pterin-free reaction are reminiscent of the peroxide-dependent oxidation of NHA (*17*, *18*). In both cases, the formation of NO^- coincides with a mixture of amino acid products. NO^- is one-electron reduced as compared with the normal NOS reaction product, •NO. Its formation in this reaction indicates that pterin-free $iNOS_{heme}$ catalyzes a two-electron oxidation of NHA rather than the three-electron oxidation observed in reactions of H_4B-bound $iNOS_{heme}$. Another difference between the reactions in the presence and absence of H_4B is evident in the stoichiometry of product formation. The maximal amount of product formed in both reactions is similar (0.75 equiv of amino acid product for the pterin-free reaction and 0.83 equiv of citrulline for the H_4B-bound reaction) and requires the addition of 2 to 2.5 electron equiv. However, titrations of pterin-free $iNOS_{heme}$ indicate that full reduction of the enzyme only requires 1 to 1.5 electrons. Product formation by pterin-free $iNOS_{heme}$ hence shows a linear dependence on the extent of reduction (see Figure 9B), but only 0.5 equiv of product is formed when $iNOS_{heme}$ is fully reduced. Additional product can be formed when excess dithionite is present in these reactions, but the stoichiometry of product formation relative to the extent of reduction provides evidence that both electrons for the oxidation of NHA by pterin-free $iNOS_{heme}$ come from dithionite. These results are consistent with the involvement of H_4B in electron transfer in NHA oxidation, as shown in Scheme 3B. The second electron, normally provided by the pterin cofactor in H_4B-bound $iNOS_{heme}$, would instead come from dithionite in the pterin-free $iNOS_{heme}$ reaction. The same tetrahedral intermediate proposed in Scheme 4 would result in both cases, but in the absence of H_4B, it would decompose to products without undergoing the proposed 1-electron oxidation by $H_3B\bullet$. The overall reaction would thus be a two-electron oxidation of NHA, with NO^- as the inorganic product. The observed products can also be explained by an indirect role for pterin in modulating whether the second electron comes from NHA (when H_4B is bound) or from dithionite or the reductase domain (in the absence of H_4B). This could be attributed to indirect effects of H_4B on the active-site structure, heme environment, or substrate binding. In particular, disruption of NHA binding would likely prevent electron transfer from NHA to the heme, thereby explaining the formation of NO^-.

The identity of the amino acid product of NHA oxidation is also different in the pterin-free reaction. The mixture of urea and cyanamide amino acid products is similar to what is observed for oxidation reactions of *N*-hydroxyguanidines catalyzed by cytochrome P450 (*77*−*79*). In these reactions, where the substrate may not be well positioned to react with $Fe^{III}O_2\bullet$ directly, oxidation is proposed to occur by reaction with superoxide dissociated from the P450 heme (*80*, *81*). The possible involvement of superoxide in the reaction of pterin-free $iNOS_{heme}$ was not investigated here, although there are conflicting reports in the literature concerning whether superoxide is involved in the oxidation of NHA catalyzed by pterin-free NOS (*75*, *82*). The active oxidant in the pterin-free reaction could also be either the $Fe^{III}OOH$ proposed for the reaction of H_4B-bound NOS with NHA or the $Fe^{V}{=}O$ species involved in arginine hydroxylation. Mechanisms to account for the formation of CN-orn have involved $Fe^{V}{=}O$, with oxygen atom insertion into the C═N bond of NHA to form an oxaziridine intermediate (*18*). However, the same oxaziridine intermediate can also be obtained following a nucleophilic reaction of $Fe^{III}OOH$ with NHA. This intermediate could subsequently break down to form citrulline, CN-orn, and NO^-, as well as a dihydroxylated product. Although the details of this reaction are not well understood, a comparison of the NHA oxidation reactions catalyzed by pterin-free $iNOS_{heme}$ and H_4B-bound $iNOS_{heme}$ suggests that they proceed by different mechanisms.

The data presented here support a role for H_4B in both steps of the NOS reaction. The absolute dependence of the first step on a redox-active, reduced pterin suggests a redox role for H_4B in the hydroxylation of arginine. Stoichiometric product formation in reactions of $iNOS_{heme}$ under conditions where a pterin radical has been directly observed provides strong evidence that H_4B is involved in electron transfer. Specifically, H_4B would provide the second electron to reduce the ferrous−dioxygen complex in the arginine reaction. This proposal is further supported by the observation that fully reduced $iNOS_{heme}$ catalyzes the formation of one equivalent of NHA in the absence of additional electrons from dithionite. H_4B is also required in the oxidation of NHA and determines the reaction products. The nature of the involvement of H_4B in this reaction is less clear, since only a small amount of pterin radical signal has been observed in the presence of NHA. The influence of H_4B on the heme redox potential, reactivity of the ferrous−dioxygen complex, NHA binding affinity and perhaps orientation, and active-site stabilization might all contribute to the effect of pterin on the reaction products. However, the role of pterin in this step is likely to also be in electron transfer, since the identity and stoichiometry of the products of the pterin-free reaction indicate that a two-electron oxidation has taken place rather than the three-electron oxidation observed when H_4B is bound. Experiments are underway to further characterize the involvement of the pterin in both steps of the NOS reaction.

ACKNOWLEDGMENT

We thank Melissa J. Clague and Kristin M. Rusche for developing the HPLC method used for pterin quantitation,

Joan M. Hevel for synthesizing $DZPH_4$, and members of the Marletta laboratory for helpful discussions.

SUPPORTING INFORMATION AVAILABLE

A gel showing the purification of $iNOS_{heme}$ (Figure S1), UV−visible spectra of oxidized and reduced forms of H_4B-bound and pterin-free $iNOS_{heme}$ (Figures S2−S4), determination of K_d values for the binding of arginine and NHA to H_4B-bound $iNOS_{heme}$ (Figures S5−S6), determination of K_d values for the binding of arginine, NHA, and $DZPH_4$ to pterin-free $iNOS_{heme}$ (Figures S7−S9), and analytical gel filtration of $iNOS_{heme}$ (Figure S10). This material is available free of charge via the Internet at http://pubs.acs.org.

REFERENCES

1. Marletta, M. A., Hurshman, A. R., and Rusche, K. M. (1998) *Curr. Opin. Chem. Biol. 2*, 656−663.
2. Marletta, M. A. (1993) *J. Biol. Chem. 268*, 12231−12234.
3. Nathan, C. (1992) *FASEB J. 6*, 3051−3064.
4. Stuehr, D. J., Kwon, N. S., Nathan, C. F., Griffith, O. W., Feldman, P. L., and Wiseman, J. (1991) *J. Biol. Chem. 266*, 6259−6263.
5. Pufahl, R. A., Nanjappan, P. G., Woodard, R. W., and Marletta, M. A. (1992) *Biochemistry 31*, 6822−6828.
6. Klatt, P., Schmidt, K., Uray, G., and Mayer, B. (1993) *J. Biol. Chem. 268*, 14781−14787.
7. Marletta, M. A. (1994) *Cell 78*, 927−930.
8. Hevel, J. M., White, K. A., and Marletta, M. A. (1991) *J. Biol. Chem. 266*, 22789−22791.
9. Stuehr, D. J., Cho, H. J., Kwon, N. S., Weise, M. F., and Nathan, C. F. (1991) *Proc. Natl. Acad. Sci. U.S.A. 88*, 7773−7777.
10. Mayer, B., John, M., Heinzel, B., Werner, E. R., Wachter, H., Schultz, G., and Böhme, E. (1991) *FEBS Lett. 288*, 187−191.
11. White, K. A., and Marletta, M. A. (1992) *Biochemistry 31*, 6627−6631.
12. Stuehr, D. J., and Ikeda-Saito, M. (1992) *J. Biol. Chem. 267*, 20547−20550.
13. McMillan, K., Bredt, D. S., Hirsch, D. J., Snyder, S. H., Clark, J. E., and Masters, B. S. (1992) *Proc. Natl. Acad. Sci. U.S.A. 89*, 11141−11145.
14. Hevel, J. M., and Marletta, M. A. (1992) *Biochemistry 31*, 7160−7165.
15. Schmidt, H. H. H. W., Smith, R. M., Nakane, M., and Murad, F. (1992) *Biochemistry 31*, 3243−3255.
16. Pufahl, R. A., and Marletta, M. A. (1993) *Biochem. Biophys. Res. Commun. 193*, 963−970.
17. Pufahl, R. A., Wishnok, J. S., and Marletta, M. A. (1995) *Biochemistry 34*, 1930−1941.
18. Clague, M. J., Wishnok, J. S., and Marletta, M. A. (1997) *Biochemistry 36*, 14465−14473.
19. Wang, C. C. Y., Ho, D. M., and Groves, J. T. (1999) *J. Am. Chem. Soc. 121*, 12094−12103.
20. Crane, B. R., Arvai, A. S., Ghosh, D. K., Wu, C., Getzoff, E. D., Stuehr, D. J., and Tainer, J. A. (1998) *Science 279*, 2121−2126.
21. Raman, C. S., Li, H., Martasek, P., Kral, V., Masters, B. S., and Poulos, T. L. (1998) *Cell 95*, 939−950.
22. Fischmann, T. O., Hruza, A., Niu, X. D., Fossetta, J. D., Lunn, C. A., Dolphin, E., Prongay, A. J., Reichert, P., Lundell, D. J., Narula, S. K., and Weber, P. C. (1999) *Nat. Struct. Biol. 6*, 233−242.
23. Li, H., Raman, C. S., Glaser, C. B., Blasko, E., Young, T. A., Parkinson, J. F., Whitlow, M., and Poulos, T. L. (1999) *J. Biol. Chem. 274*, 21276−21284.
24. Tierney, D. L., Huang, H., Martasek, P., Masters, B. S., Silverman, R. B., and Hoffman, B. M. (1999) *Biochemistry 38*, 3704−3710.
25. Tierney, D. L., Huang, H., Martasek, P., Roman, L. J., Silverman, R. B., Masters, B. S. S., and Hoffman, B. M. (2000) *J. Am. Chem. Soc. 122*, 5405−5406.
26. Crane, B. R., Arvai, A. S., Ghosh, S., Getzoff, E. D., Stuehr, D. J., and Tainer, J. A. (2000) *Biochemistry 39*, 4608−4621.
27. Tayeh, M. A., and Marletta, M. A. (1989) *J. Biol. Chem. 264*, 19654−19658.
28. Kwon, N. S., Nathan, C. F., and Stuehr, D. J. (1989) *J. Biol. Chem. 264*, 20496−20501.
29. Baek, K. J., Thiel, B. A., Lucas, S., and Stuehr, D. J. (1993) *J. Biol. Chem. 268*, 21120−21129.
30. Abu-Soud, H. M., Loftus, M., and Stuehr, D. J. (1995) *Biochemistry 34*, 11167−11175.
31. Klatt, P., Schmidt, K., Lehner, D., Glatter, O., Bachinger, H. P., and Mayer, B. (1995) *EMBO J. 14*, 3687−3695.
32. Klatt, P., Schmid, M., Leopold, E., Schmidt, K., Werner, E. R., and Mayer, B. (1994) *J. Biol. Chem. 269*, 13861−13866.
33. White, K. A. (1994) Doctoral Thesis, The University of Michigan, Ann Arbor, MI.
34. Rodriguez-Crespo, I., Gerber, N. C., and Ortiz de Montellano, P. R. (1996) *J. Biol. Chem. 271*, 11462−11467.
35. Rusche, K. M., Spiering, M. M., and Marletta, M. A. (1998) *Biochemistry 37*, 15503−15512.
36. Presta, A., Weber-Main, A. M., Stankovich, M. T., and Stuehr, D. J. (1998) *J. Am. Chem. Soc. 120*, 9460−9465.
37. Werner, E. R., Pitters, E., Schmidt, K., Wachter, H., Werner-Felmayer, G., and Mayer, B. (1996) *Biochem. J. 320*, 193−196.
38. Mayer, B., Wu, C., Gorren, A. C., Pfeiffer, S., Schmidt, K., Clark, P., Stuehr, D. J., and Werner, E. R. (1997) *Biochemistry 36*, 8422−8427.
39. Pfeiffer, S., Gorren, A. C., Pitters, E., Schmidt, K., Werner, E. R., and Mayer, B. (1997) *Biochem. J. 328*, 349−352.
40. Bec, N., Gorren, A. C., Voelker, C., Mayer, B., and Lange, R. (1998) *J. Biol. Chem. 273*, 13502−13508.
41. Hurshman, A. R., Krebs, C., Edmondson, D. E., Huynh, B. H., and Marletta, M. A. (1999) *Biochemistry 38*, 15689−15696.
42. Di Iorio, E. E. (1981) *Methods Enzymol. 76*, 57−72.
43. Richards, M. K. (1995) Doctoral Thesis, The University of Michigan, Ann Arbor, MI.
44. Pfleiderer, W. (1985) in *Folates and Pterins* (Blakely, R. L., and Benkovic, S. J., Eds.) pp 43−114, John Wiley and Sons, New York.
45. Brenneman, A. R., and Kaufman, S. (1964) *Biophys. Res. Commun. 17*, 177.
46. Moad, G., Luthy, C. L., Benkovic, P. A., and Benkovic, S. J. (1979) *J. Am. Chem. Soc. 101*, 6068−6076.
47. Brandish, P. E., Buechler, W., and Marletta, M. A. (1998) *Biochemistry 37*, 16898−16907.
48. Howells, D. W., Smith, I., and Hyland, K. (1986) *J. Chromatogr. 381*, 285−294.
49. Howells, D. W., and Hyland, K. (1987) *Clin. Chim. Acta 167*, 23−30.
50. de Montigny, P., Stobaugh, J. F., Givens, R. S., Carlson, R. G., Srinivasachar, K., Sternson, L. A., and Higuchi, T. (1987) *Anal. Chem. 59*, 1096−1101.
51. Green, L. C., Wagner, D. A., Glogowski, J., Skipper, P. L., Wishnok, J. S., and Tannenbaum, S. R. (1982) *Anal. Biochem. 126*, 131−138.
52. Ghosh, D. K., Wu, C., Pitters, E., Moloney, M., Werner, E. R., Mayer, B., and Stuehr, D. J. (1997) *Biochemistry 36*, 10609−10619.
53. Miller, R. T., Martasek, P., Raman, C. S., and Masters, B. S. (1999) *J. Biol. Chem. 274*, 14537−14540.
54. Hemmens, B., Goessler, W., Schmidt, K., and Mayer, B. (2000) *J. Biol. Chem. 275*, 35786−35791.
55. Klatt, P., Pfeiffer, S., List, B. M., Lehner, D., Glatter, O., Bachinger, H. P., Werner, E. R., Schmidt, K., and Mayer, B. (1996) *J. Biol. Chem. 271*, 7336−7342.

56. List, B. M., Klosch, B., Volker, C., Gorren, A. C., Sessa, W. C., Werner, E. R., Kukovetz, W. R., Schmidt, K., and Mayer, B. (1997) *Biochem. J. 323*, 159−165.
57. Xie, Q. W., Leung, M., Fuortes, M., Sassa, S., and Nathan, C. (1996) *Proc. Natl. Acad. Sci. U.S.A. 93*, 4891−4896.
58. Presta, A., Siddhanta, U., Wu, C., Sennequier, N., Huang, L., Abu-Soud, H. M., Erzurum, S., and Stuehr, D. J. (1998) *Biochemistry 37*, 298−310.
59. Abu-Soud, H. M., Wu, C., Ghosh, D. K., and Stuehr, D. J. (1998) *Biochemistry 37*, 3777−3786.
60. Gorren, A. C., List, B. M., Schrammel, A., Pitters, E., Hemmens, B., Werner, E. R., Schmidt, K., and Mayer, B. (1996) *Biochemistry 35*, 16735−16745.
61. Sono, M., Ledbetter, A. P., McMillan, K., Roman, L. J., Shea, T. M., Masters, B. S. S., and Dawson, J. H. (1999) *Biochemistry 38*, 15853−15862.
62. Rusche, K. M., and Marletta, M. A. (2001) *J. Biol. Chem. 276*, 421−427.
63. Rusche, K. M. (1998) Doctoral Thesis, The University of Michigan, Ann Arbor, MI.
64. Kohout, F. C., and Lampe, F. W. (1967) *J. Chem. Phys. 46*, 4075−4084.
65. Bazylinski, D. A., and Hollocher, T. C. (1985) *Inorg. Chem. 24*, 4285−4288.
66. Boggs, S., Huang, L., and Stuehr, D. J. (2000) *Biochemistry 39*, 2332−2339.
67. Benkovic, S. J. (1980) *Ann. Rev. Biochem. 49*, 227−251.
68. Kappock, T. J., and Caradonna, J. P. (1996) *Chem. Rev. 96*, 2659−2756.
69. Chen, D., and Frey, P. A. (1998) *J. Biol. Chem. 273*, 25594−25601.
70. Francisco, W. A., Tian, G., Fitzpatrick, P. F., and Klinman, J. P. (1998) *J. Am. Chem. Soc. 120*, 4057−4062.
71. Riethmuller, C., Gorren, A. C., Pitters, E., Hemmens, B., Habisch, H. J., Heales, S. J., Schmidt, K., Werner, E. R., and Mayer, B. (1999) *J. Biol. Chem. 274*, 16047−16051.
72. Werner, E. R., Habisch, H. J., Gorren, A. C., Schmidt, K., Canevari, L., Werner-Felmayer, G., and Mayer, B. (2000) *Biochem. J. 348 Pt 3*, 579−583.
73. Bec, N., Gorren, A. F. C., Mayer, B., Schmidt, P. P., Andersson, K. K., and Lange, R. (2000) *J. Inorg. Biochem. 81*, 207−211.
74. Wei, C. C., Wang, Z. Q., Wang, Q., Meade, A. L., Hemann, C., Hille, R., and Stuehr, D. J. (2001) *J. Biol. Chem. 276*, 315−319.
75. Adak, S., Wang, Q., and Stuehr, D. J. (2000) *J. Biol. Chem. 275*, 33554−33561.
76. Gorren, A. C., Bec, N., Schrammel, A., Werner, E. R., Lange, R., and Mayer, B. (2000) *Biochemistry 39*, 11763−11770.
77. Boucher, J. L., Genet, A., Vadon, S., Delaforge, M., Henry, Y., and Mansuy, D. (1992) *Biochem. Biophys. Res. Commun. 187*, 880−886.
78. Renaud, J. P., Boucher, J. L., Vadon, S., Delaforge, M., and Mansuy, D. (1993) *Biochem. Biophys. Res. Commun. 192*, 53−60.
79. Jousserandot, A., Boucher, J.-L., Desseaux, C., Delaforge, M., and Mansuy, D. (1995) *Bioorg. Med. Chem. Lett. 5*, 423−426.
80. Mansuy, D., Boucher, J. L., and Clement, B. (1995) *Biochimie 77*, 661−667.
81. Jousserandot, A., Boucher, J. L., Henry, Y., Niklaus, B., Clement, B., and Mansuy, D. (1998) *Biochemistry 37*, 17179−17191.
82. Moali, C., Boucher, J. L., Renodon-Corniere, A., Stuehr, D. J., and Mansuy, D. (2001) *Chem. Res. Toxicol. 14*, 202−210.

BI012002H